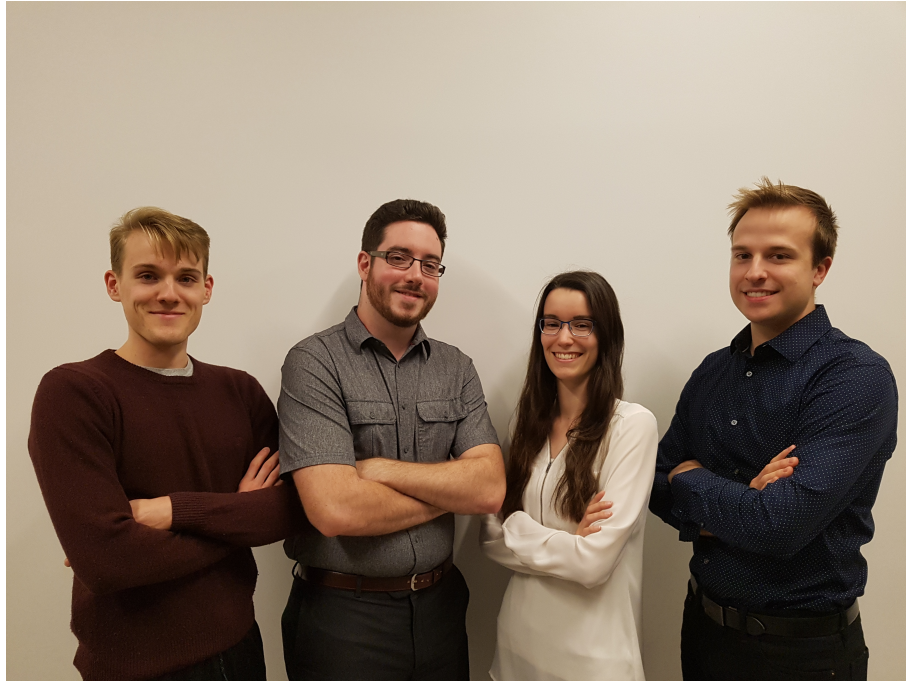


Waterfront 2A - Modelling Report
MCG4322



Waterfront Robot 2A

Marc-André Arsenault (8172498)

Mathieu Carroll (8089784)

Alexane Lahaie (8204533)

Joshua O'Reilly (8359885)

University of Ottawa
Department of Mechanical Engineering
October 02, 2019

Contents

List of Figures	iii
List of Tables	iii
1 Project Charter	1
1.1 Mandate	1
1.2 Requirements	1
1.3 Constraints	1
1.4 Criteria	1
1.5 Parametrization Outline	1
2 Design Solution	2
3 Assumptions and Approximations	5
3.1 Tibia Simplification During Analysis	5
3.2 Friction	6
3.3 Nominal and Actual Values for Motors	6
4 Component Properties	8
4.1 Robot General Dimensions	8
4.2 Battery Requirements and Dimensions	9
4.3 Centre of Mass	10
5 Kinematics and Applied Forces	13
5.1 Normal Forces at Feet	13
5.2 Static Moment at Leg Joints	14
5.3 Generalized Dynamic Equation of Motion	16
5.4 Stability Analysis and Slopes	19
5.5 Drag Force from Wind	24
6 References	27
Appendix A Additional Material	29
A.1 Mass Moment of Inertia of Square Tube	29
A.2 Generalized Equation of Motion	32
A.3 Force at Feet	35

A.4 Drag Coefficients	35
A.5 Battery Sample Code	37
A.6 Centre of Mass Calculation	38
Appendix B Data Sheets	38

List of Figures

1	Crab Top View	2
2	Crab Leg Side View	3
3	Crab Knee Top View	3
4	Crab Hip Top View	4
5	Crab Hip Section View	4
6	Crab Straight Leg Assumption	6
7	Crab General Dimensions	8
8	Layout of Components in Robot Chassis	11
9	FBD of Whole Robot	13
10	FBD of Tibia Member	15
11	FBD of Whole Leg	15
12	Side View of Leg i	17
13	Centre of Mass and Diamond Shaped Stability Area	19
14	Rotation Around X by 20°	21
15	Rotation Around X by -20°	22
16	Rotation Around Y by 57°	23
17	Rotation Around Y by -73°	24
18	FBD of Whole Robot on a Slope	26
19	Drag Force Worst Case Scenario	26
20	Mass Moment of Inertia of Cylindrical Tube	29
21	Mass Moment of Inertia of Square Tube	30
22	Mass Moment of Inertia of Square Tube - Slab view	30
23	Side View of Leg i	32
24	Simplification Steps for Inertia Matrix	34
25	Various Drag Coefficients for Two-Dimensional Objects [9]	36

List of Tables

1	Assumptions Made During Robot Modelling	5
2	Motors Used for Power and Weight Approximations	7
3	Harmonic Drives Used for Power and Weight Approximations	7
4	General Dimensions	9
5	Leg Joint Torques Based on Two Different Calculated Normal Forces	16

6	Leg Joint Torque Based on Generalized Equation of Motion with Forward Acceleration	18
7	Leg Joint Torque Based on Generalized Equation of Motion with Backward Acceleration	18
8	Centre of Mass Calculation and Components' Location	38

1 Project Charter

1.1 Mandate

Group WR2A is mandated to develop a rugged device which uses a biomimetic inspired locomotion system to remove waste from waterfronts. It must be self-reliant and be resistant to exterior environments such as areas with minimal accessibility, and rough weather and terrain.

1.2 Requirements

The design is to be solar powered and have a biomimetic inspired locomotion system. It must operate in rain, water, high heat, and, and navigate terrain such as sand, mud, plants and bramble. Human intervention should only be necessary to empty the litter container. It should resist vandalism. The litter collector size will vary from one to 5000 cm³ and one to 5 kg.

1.3 Constraints

The only constraint is that the device should not have any continuously rotating joints; due to the relatively new technology, the rest of the project is left open-ended.

1.4 Criteria

Power consumption per kilogram (device and litter) should be minimized. The operating time should be maximized for better litter collection efficiency. The robot's capacity to navigate a variety of environments, including sand and pebble beaches, shallow water, mud and around small plants, should be maximized. The mechanical stability and agility of the robot should be optimized as well to permit a reasonable turning radius and ability to navigate on inclinations. Finally, aesthetics should be considered as it will operate in public spaces.

1.5 Parametrization Outline

Input parameters that modify the design include the maximum litter weight, maximum litter volume, litter dimensions as per Group WR2B, battery life without recharging, and maximum forward velocity.

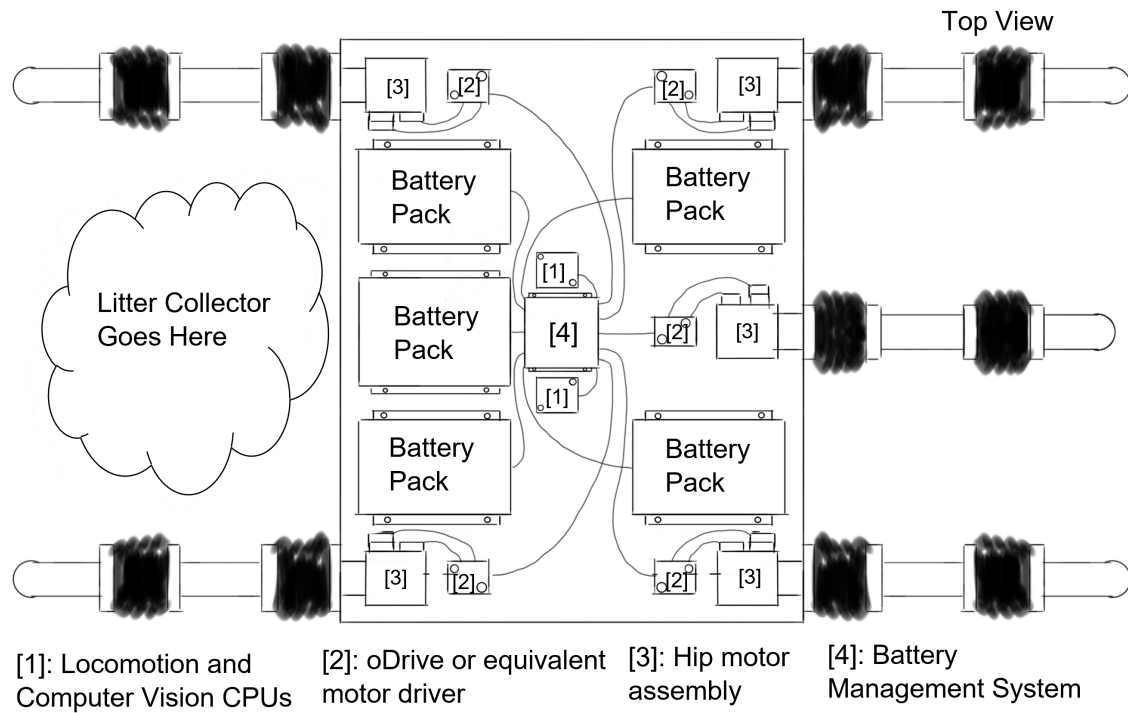


Figure 1: Crab Top View

2 Design Solution

Most drawings have not been updated from the Concepts Report. These will be modified for the Design Dossier. Ultimately, the modifications are purely internal and will not influence the external kinematic analysis. The only major change was the distribution of components within the chassis, in order to calculate a more adequate centre of mass. The arrangement in Figure 1 is thus replaced by the arrangement shown further on in Figure 8.

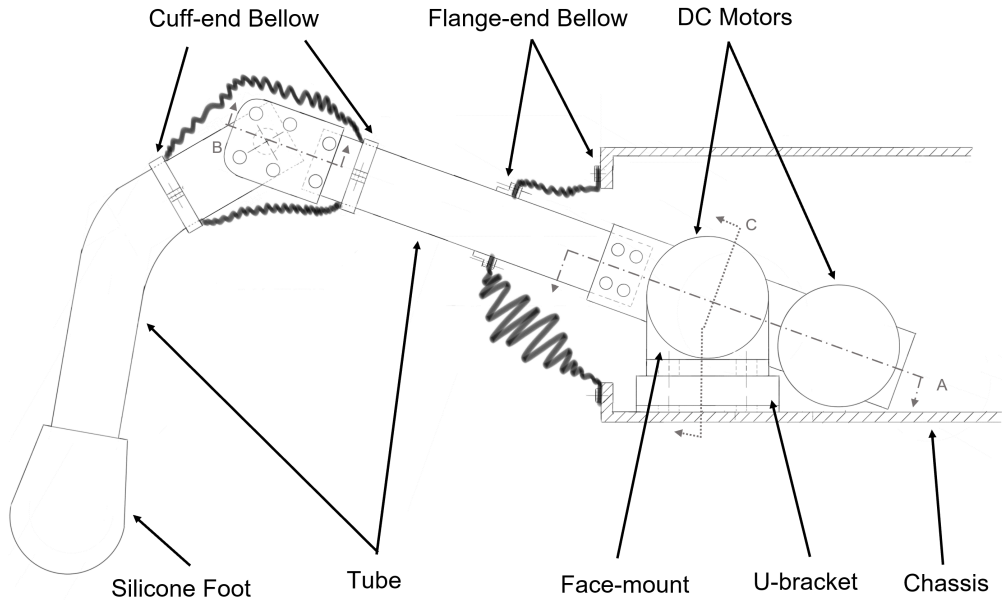


Figure 2: Crab Leg Side View

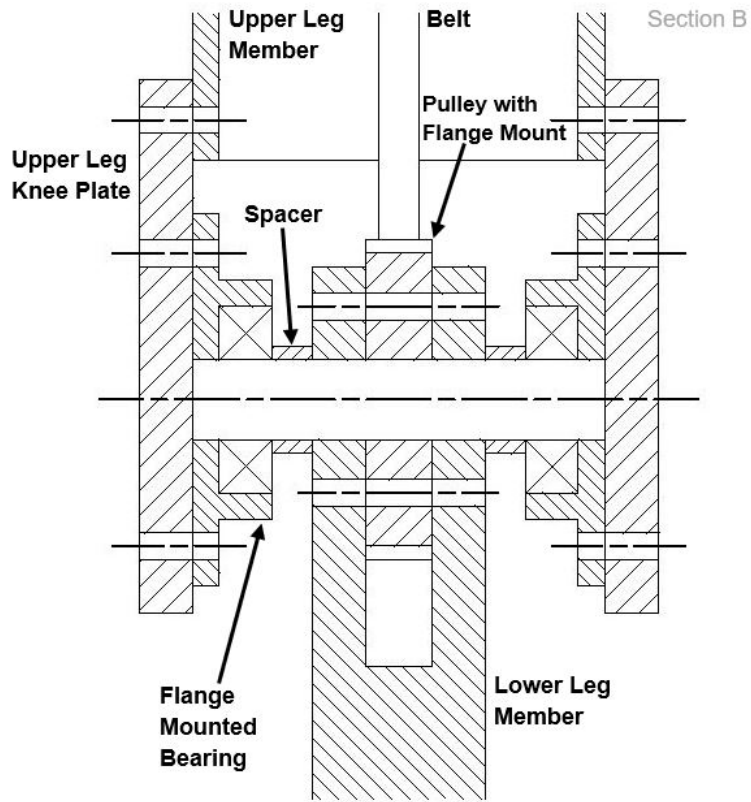


Figure 3: Crab Knee Top View

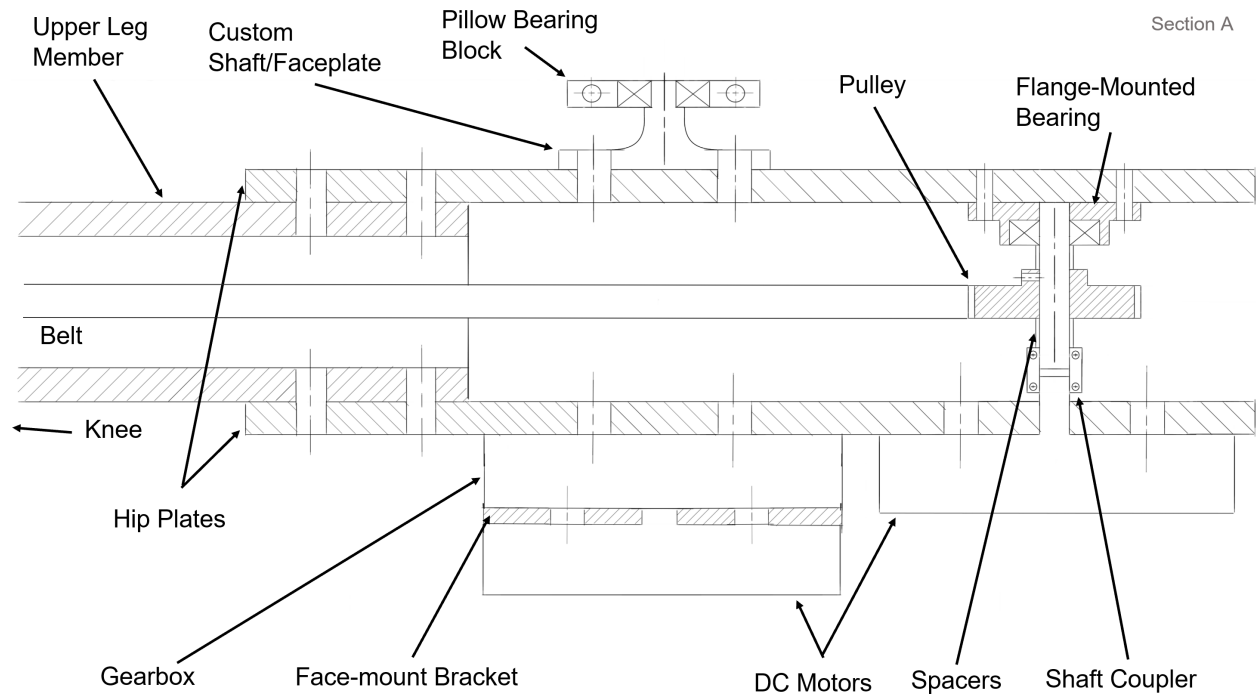


Figure 4: Crab Hip Top View

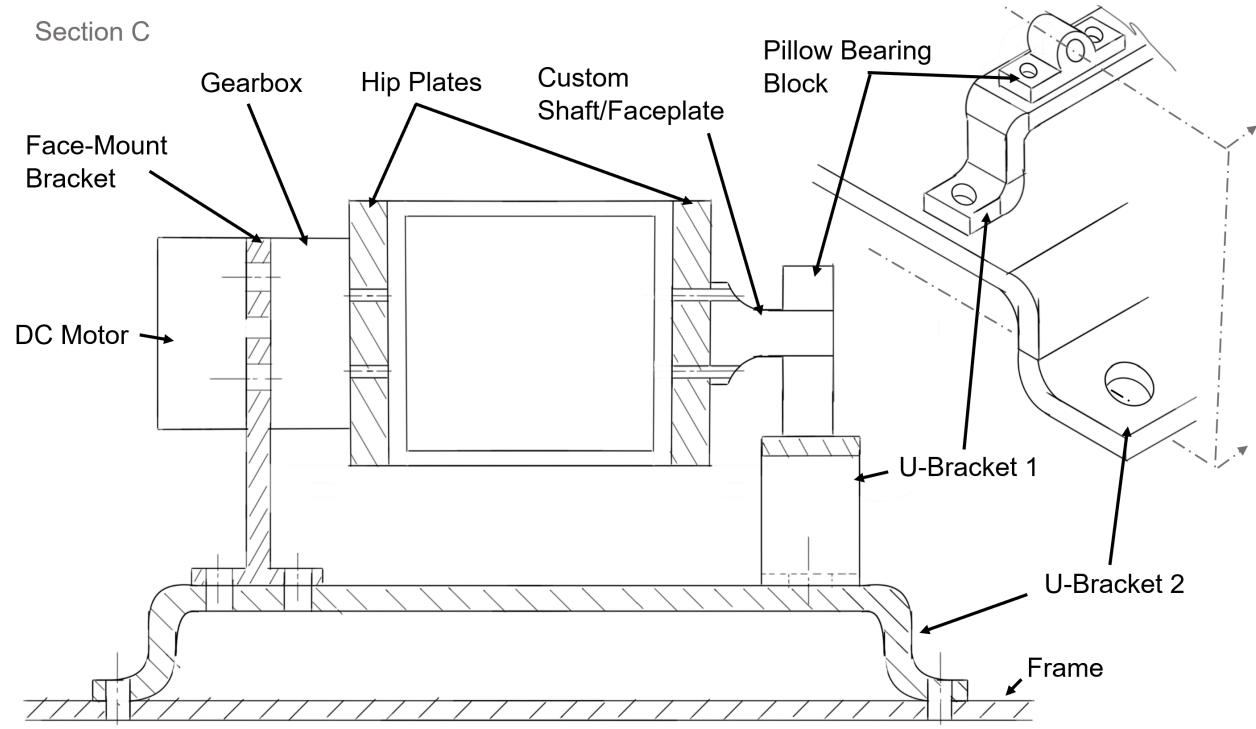


Figure 5: Crab Hip Section View

3 Assumptions and Approximations

Table 1 contains some assumptions and approximations about the working conditions and applied loads.

Table 1: Assumptions Made During Robot Modelling

Assumption Type	Assumption
Hip Range of Motion	0° (horizontal) to 30°
Knee Range of Motion	Foot no further inwards than knee
Maximum wind speed	73 km/h (Ottawa, September 2018 Tornadoes)
Linkage composition	Homogeneous rigid bodies
Terrain	Sand, pebble, shallow water (under chassis), mud, small plants
Environment	Salt, dust, high heat, humidity

The first two assumptions relate to the mechanical stability of the robot. It is more stable when the body is closer to the ground, and when it has a wider base. The first assumption stipulates that, during operation, the hip joint will allow the thigh to turn between horizontal and 30 degrees above horizontal, keeping the body lower than if a negative angle was selected. The second states that the foot will extend beyond the thigh, but will never retract closer than the knee, since it will require more torque to counter-balance an external force, making it less stable. A maximum value was selected for wind speed based on Ottawa peak wind speeds (including the tornado events). It is assumed that the robot would not be left operating in more extreme weather, such as hurricanes. Other assumptions are based on basic simplification of the calculations or on the given requirements.

3.1 Tibia Simplification During Analysis

As seen in the concept image in Figure 2, the tibia linkage is to have a bend. This will help reduce the angle at the knee for the bellows. However, for the force analysis, the shin was simplified as a simple line joining each end of the member. This is shown as the dashed line in Figure 6.

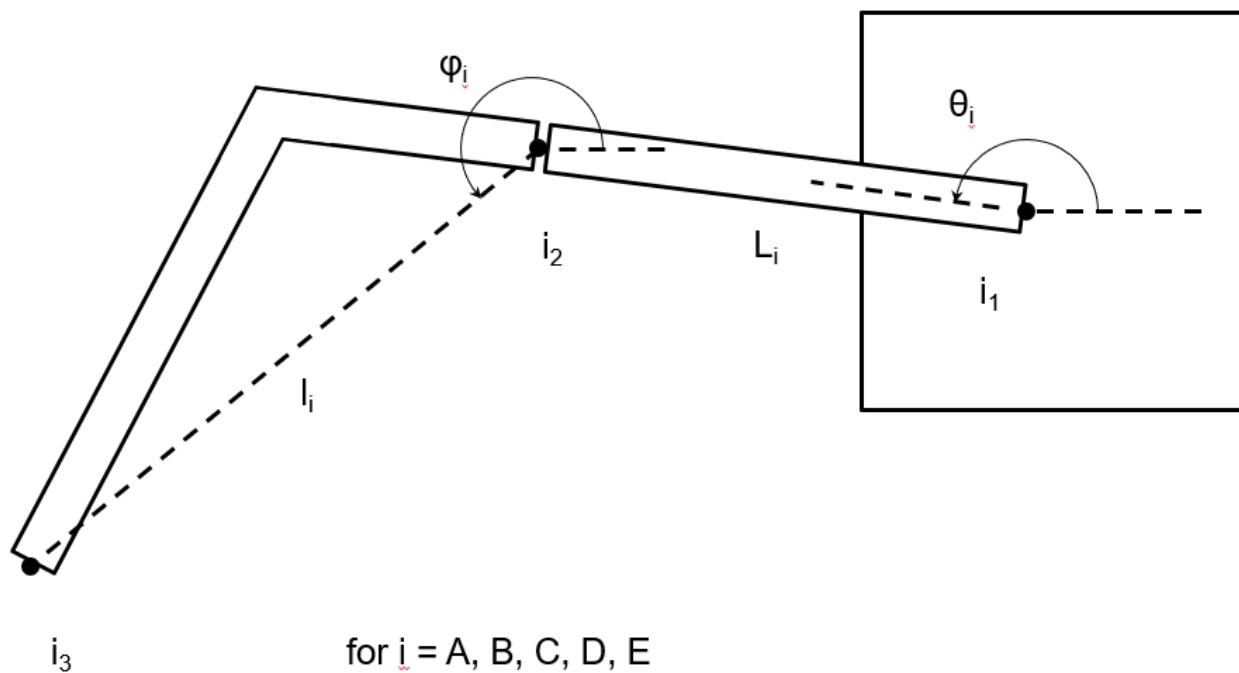


Figure 6: Crab Straight Leg Assumption

3.2 Friction

The friction force is shown in all FBDs. However, in the calculations without slope, these were assumed to be negligible compared to the normal forces at the feet. The friction forces only come into effect when the robot is on a slope. However, the calculated slope in terms of stability is relatively small and thus friction is assumed to have little impact in this case. This assumption is further supported by the fact that the robot legs will dig into the sand, mud or pebbles to a certain extent. This would create additional normal forces on the side of the foot, preventing the robot from slipping easily.

3.3 Nominal and Actual Values for Motors

The approximate weights and power usage of the motors were inspired by existing harmonic drive and motor models. The characteristics of the observed models are shown in Tables 2 and 3, and datasheets are included in Appendix B[1] [2].

Table 2: Motors Used for Power and Weight Approximations

Properties	Hip Motor	Knee Motor
Manufacturer	Maxon	Maxon
Model	EC 90 Flat	EC 60 Flat
Weight [kg]	0.98	0.36
Diameter [mm]	90	60
Voltage [V]	48	48
Nominal Current [A]	4.06	4.6
Nominal Torque [mNm]	964	577
Stall Torque [Nm]	13.1	4.87

Table 3: Harmonic Drives Used for Power and Weight Approximations

Properties	Hip Harmonic Drive	Knee Harmonic Drive
Manufacturer	Harmonic Drive	Harmonic Drive
Model	FB-40-100-2-GR	FB-25-100-2-GR
Reduction Ratio	100	100
Weight [kg]	1.8	0.5
Diameter [mm]	135	85
Rated Torque [Nm]	157	39
Average Torque Limit [Nm]	186	52
Momentary Peak Torque [Nm]	343	91

Calculations were based when possible on nominal or rated torque values, to make them correspond to the calculated moments at the joints. However, as this analysis takes into account the worse case scenarios for the robot, it must be understood that the motors will not always be operating at their nominal point. These occurrences would happen on rare or momentary occasions. Thus, in those cases the average torque limit or momentary peak torque are considered. The harmonic drives FB-series are also non-backdrivable; when the robot is stationary, the harmonic drives will take the static torque, significantly reducing the power drawn from the motors.

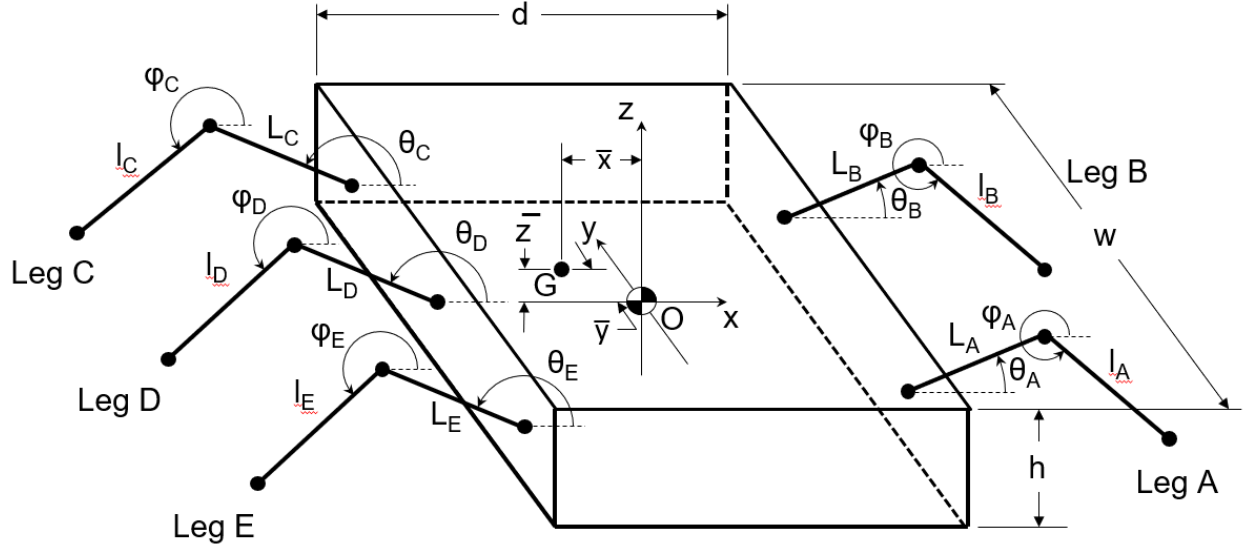


Figure 7: Crab General Dimensions

4 Component Properties

4.1 Robot General Dimensions

Figure 7 shows the general dimensional parameters of the robot. The center of origin is currently located in the geometric center of the chassis in x and y directions and at the bottom of the chassis in z . The crab consists of five legs named from A to E. The lengths of the thigh members and tibia members are identified with L_i and l_i respectively, where $i = A, B, C, D, \text{ or } E$. Similarly, the angles of the thigh members are identified with θ_i , whereas the angles of the tibia members are identified with ϕ_i . Both of these angles are measured from the global positive x -axis in the xz -plane. Each node of the leg is identified by the letter of the leg (A to E) followed by an index of 1, 2 or 3 representing the hip, knee, and foot respectively.

Table 4 shows the values chosen for each parameter. The leg angles were chosen to represent the worst case of leg positioning for the robot. This is limited due to the fact that each joint will have a bellow cover, making the possible motion smaller. Chassis size was determined based on the component layout determined in the center of mass analysis.

Table 4: General Dimensions

Variable	Value	Unit	Variable	Value	Unit
φ_A	315	Degrees	l_A	300	mm
φ_B	315	Degrees	l_B	300	mm
φ_C	225	Degrees	l_C	300	mm
φ_D	225	Degrees	l_D	300	mm
φ_E	225	Degrees	l_E	300	mm
θ_A	0	Degrees	\bar{x}	-72	mm
θ_B	0	Degrees	\bar{y}	0	mm
θ_C	180	Degrees	\bar{z}	71	mm
θ_D	180	Degrees	d	600	mm
θ_E	180	Degrees	w	1000	mm
L_A	300	mm	h	200	mm
L_B	300	mm			
L_C	300	mm			
L_D	300	mm			
L_E	300	mm			

4.2 Battery Requirements and Dimensions

Cells are arranged into a battery and managed by a Battery Management System [3]. All electronics are powered from this with the necessary voltage regulators. The battery voltage is defined as the highest voltage of any component, V_{max} , likely the motors running between 24 and 48 V. The number of battery cells running in series, N_{series} , is defined as

$$N_{series} = \frac{V_{max}}{V_{cell}} = \frac{V_{max}}{3.6V} \quad (1)$$

The number of cells in parallel, $N_{parallel}$, to achieve the desired run time is defined as

$$N_{parallel} = \frac{T \cdot I}{Q} = \frac{[h] \cdot [A]}{[Ah]} \quad (2)$$

where T is the runtime in hours, I is the total current draw of the robot and Q is the Amp-hour rating of an individual battery cell [4].

The total number of required cells is the number of series cells multiplied by the number of parallel cells.

$$N = N_{parallel} \cdot N_{series} \quad (3)$$

As an example, a tested configuration included a Maxon Motor EC90 260W and Maxon Motor EC60 200W per leg, Panasonic NCR18650B cells in the battery, as well as very

conservative estimates for the power consumption of Group WR2Bs litter picker [2] [1] [5] [6]. The total current draw is 80 A, with a motor voltage of 48 V. The number of cells in series is thus

$$N_{series} = \frac{48V}{3.6V} = 13.33\text{cells} \quad (4)$$

This is rounded up the 14 cells in series. The number of cells in parallel is calculated in the same way

$$N_{parallel} = \frac{2\text{hours} \cdot 80A}{3.4Ah} = 47.05\text{cells} \quad (5)$$

Again, this value is rounded up to 48 cells. Finally, the total number of required cells in calculated

$$N = 14 \cdot 48 = 672 \quad (6)$$

These cells could be split up into multiple batteries, or take different shapes and sizes. An example script is found in Appendix A.5 and gives one large battery that contains vertically aligned cells with as-close-to-square-as-possible width and length. In contrast, for the purpose of determining an approximate centre of mass, the cells were separated into four equal batteries in the center of mass calculation presented in Section 4.3.

4.3 Centre of Mass

The centre of mass was calculated with the following steps:

- Assuming a total robot mass (namely assuming battery mass).
- Calculating required motor torques and selecting appropriate motors and harmonic drives.
- Calculating required battery size with motor and electronics power requirements.
- Making a layout of the components (legs, batteries, other groups' litter picker, etc.) within the chassis and determining their distance from the origin in the middle of the chassis.
- Calculating the centre of mass.
- Iterate.

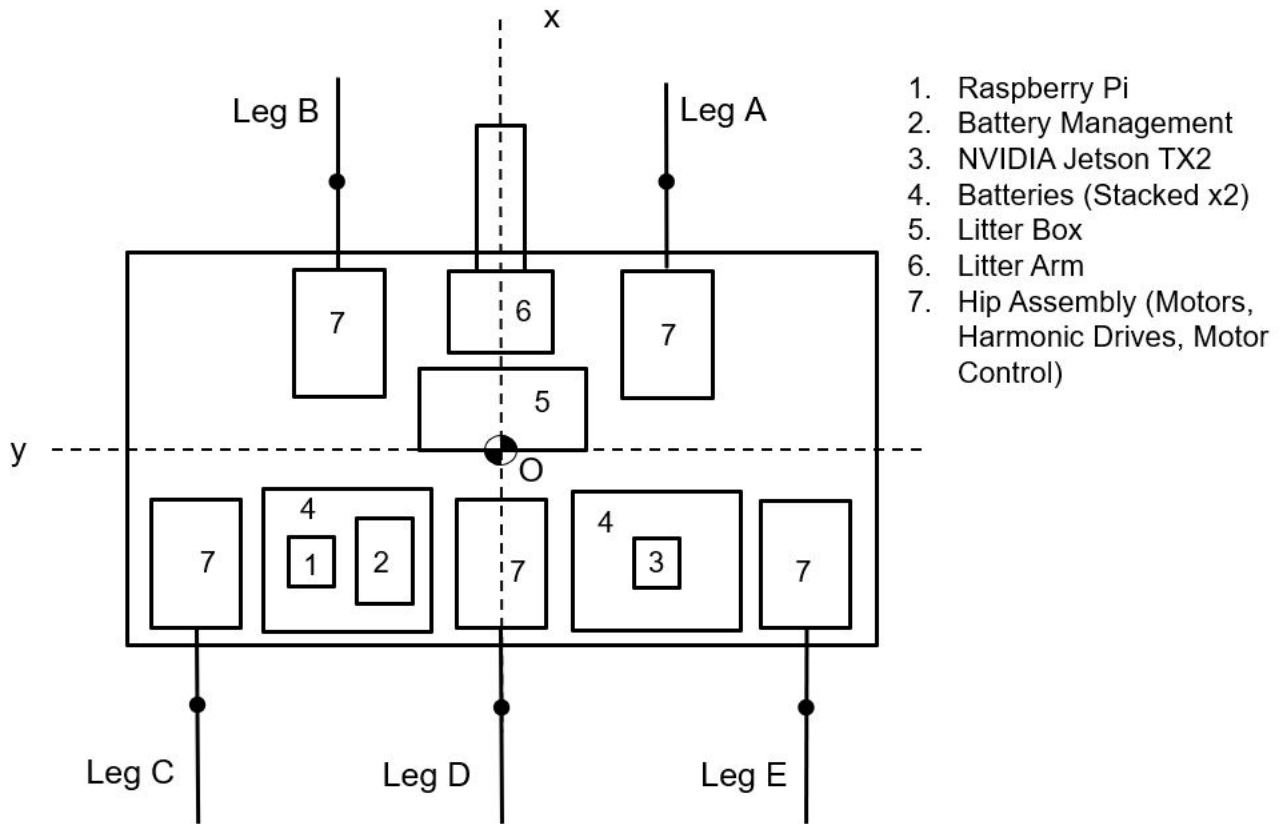


Figure 8: Layout of Components in Robot Chassis

The first iteration was done by assuming an equal normal force acting on all legs of the robot, as the centre of mass is ultimately required to get more precise normal forces (see equations for normal forces in Section 5.1). These more precise normal forces were then used in the next iteration to get more extreme torques.

The component layout was drafted based on the size and weight of the various components. Figure 8 shows the general arrangement of components. The centre of mass of each component was assumed at its middle. The specific location coordinates were specified in an excel table (see Appendix A.6), which took all components into consideration for the centre of mass calculation. The general chassis dimensions were also calculated as a consequence of this calculation.

The centre of mass is given by the following equation.

$$x_{cm} = \frac{\sum m_i x_i}{\sum m_i} \quad y_{cm} = \frac{\sum m_i y_i}{\sum m_i} \quad z_{cm} = \frac{\sum m_i z_i}{\sum m_i} \quad (7)$$

where m_i are the mass of various components and x_i , y_i and z_i are the distance of the centre of mass of each component compared to the origin of the robot, on each axis. The centre of mass value is used to assess the stability of the robot in Section 5.4.

5 Kinematics and Applied Forces

5.1 Normal Forces at Feet

The normal forces acting on the robot are shown in Figure 9. The 5 legged robot is considered a statically indeterminate (hyperstatic) case (as determined from the original equations shown in Appendix A.3). Thus it is impossible to mathematically determine the resulting force at every foot of the robot without considering bending in the robot's material.

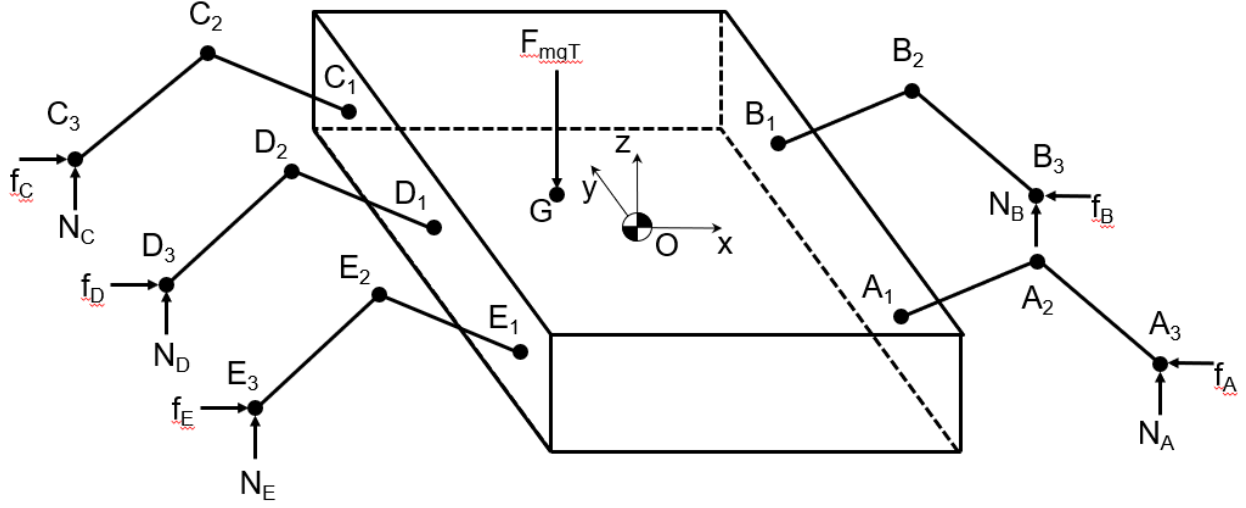


Figure 9: FBD of Whole Robot

In order to calculate realistic (worst case) values of torque, the reaction forces at the robot's feet were calculated for two possible solutions where only three feet would touch the ground.

The 2 combinations of feet touching the ground are: 1. A, C, D and 2. B, D, E. To simplify calculations and algebra, a matrix system approach was used.

For combination 1., the sum of forces and moments are given by

$$\sum F_z = 0 = N_A + N_C + N_D - F_{mgT} \quad (8)$$

$$\sum M_{A_x} = 0 = N_C r_{ca_y} + N_D r_{da_y} - F_{mgT} r_{ga_y} \quad (9)$$

$$\sum M_{C_y} = 0 = -N_A r_{ac_x} - N_D r_{dc_x} + F_{mgT} r_{gc_x} \quad (10)$$

For combination 2., the sum of forces and moments are given by

$$\sum F_z = 0 = N_B + N_D + N_E - F_{mgT} \quad (11)$$

$$\sum M_{B_x} = 0 = -N_D r_{db_y} - N_E r_{eb_y} + F_{mgT} r_{gb_y} \quad (12)$$

$$\sum M_{E_y} = 0 = -N_B r_{be_x} - N_D r_{de_x} + F_{mgT} r_{ge_x} \quad (13)$$

where the r values represent the distance between the foot and the reference point, perpendicular to the rotation axis.

The following is an example with combination 1. A matrix solver is used to find reaction values.

$$\begin{aligned} \begin{bmatrix} N_A \\ N_C \\ N_D \end{bmatrix} &= \begin{bmatrix} 1 & 1 & 1 \\ 0 & r_{ca_y} & r_{da_y} \\ r_{ac_x} & r_{dc_x} & 0 \end{bmatrix}^{-1} \begin{bmatrix} F_{mgT} \\ F_{mgT} r_{ga_y} \\ F_{mgT} r_{gc_x} \end{bmatrix} \\ &= \begin{bmatrix} 1 & 1 & 1 \\ 0 & 600mm & 200mm \\ 1624mm & 0 & 0 \end{bmatrix}^{-1} \begin{bmatrix} 625N \\ 124978Nmm \\ 462656Nmm \end{bmatrix} = \begin{bmatrix} 285N \\ 142N \\ 198N \end{bmatrix} \end{aligned} \quad (14)$$

5.2 Static Moment at Leg Joints

The forces acting on the tibia member are shown in Figure 10.

This allows the knee joint moment to be calculated using the following equation.

$$\sum M_{i_2} = 0 = N_i l_i \cos \phi_i - M_{i_2} \quad (15)$$

$$M_{i_2} = N_i l_i \cos \phi_i \quad (16)$$

An example for the knee joint moment calculation of leg A, using the worst case normal force is as follows:

$$\sum M_{A_2} = 0 = N_A l_A \cos \phi_A - M_{A_2} \quad (17)$$

$$M_{A_2} = N_A l_A \cos \phi_A = (285N)(300mm)(\cos(315^\circ)) = 60,423 \text{ Nmm} \quad (18)$$

The forces acting on the leg (including the tibia and thigh members) are shown in Figure 11.

This allows the hip joint moment to be calculated using the following equation.

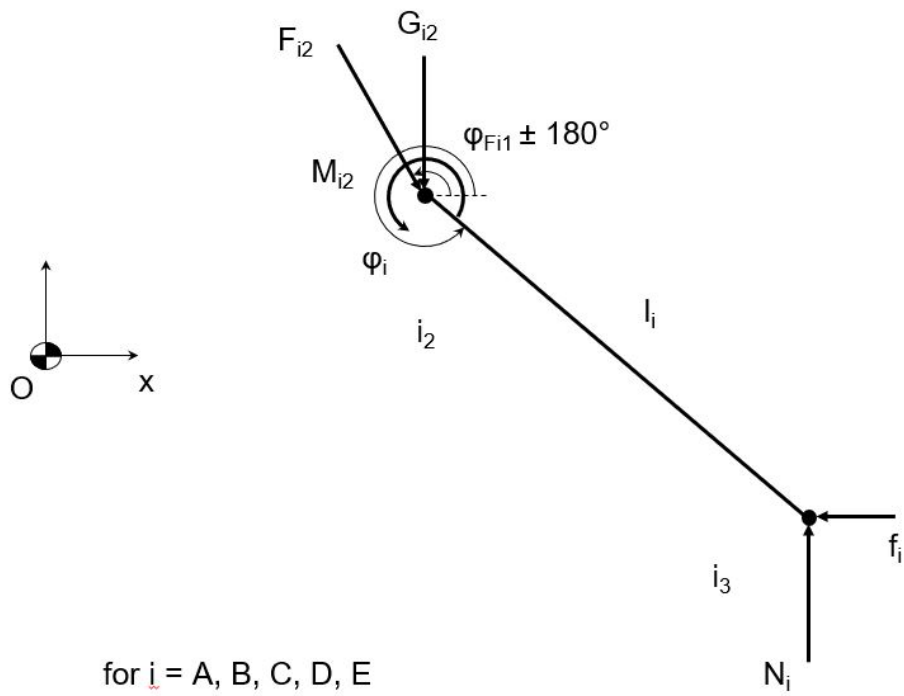


Figure 10: FBD of Tibia Member

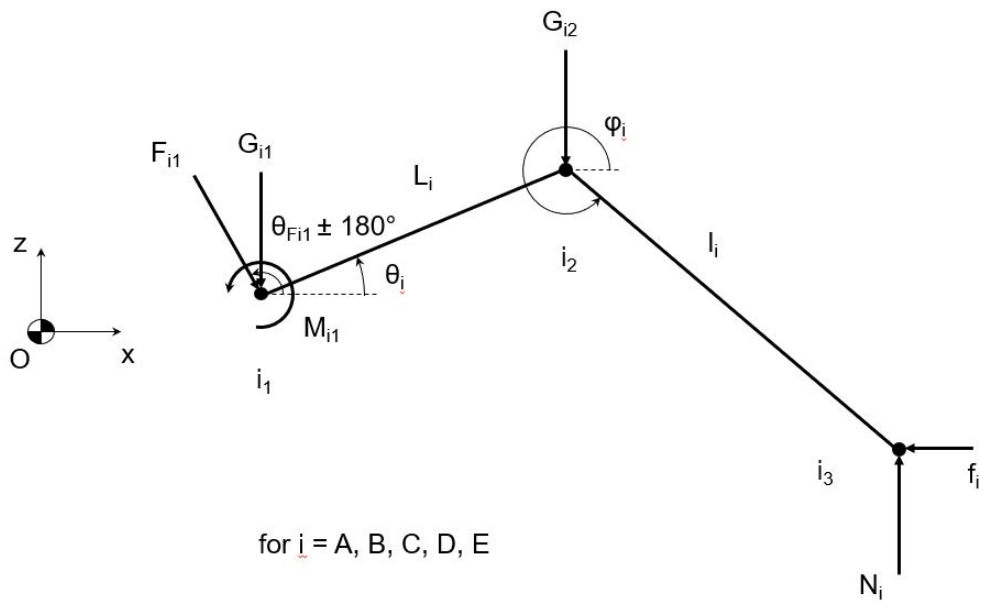


Figure 11: FBD of Whole Leg

$$\sum M_{i_1} = 0 = N_i[L_i \cos \theta_i + l_i \cos \phi_i] - G_{i2}L_i \cos \theta_i - M_{i_1} \quad (19)$$

$$M_{i_1} = N_i[L_i \cos \theta_i + l_i \cos \phi_i] - G_{i2}L_i \cos \theta_i \quad (20)$$

An example for the hip joint moment calculation of leg A, using the worst case normal force is as follows:

$$\sum M_{A_1} = 0 = N_A[L_A \cos \theta_A + l_A \cos \phi_A] - G_{i2}L_A \cos \theta_A - M_{A_1} \quad (21)$$

$$\begin{aligned} M_{A_1} &= N_A[L_A \cos \theta_A + l_A \cos \phi_A] - G_{i2}L_A \cos \theta_A \\ &= (285\text{N})[(300\text{mm}) \cos (0^\circ) + (300\text{mm}) \cos (315^\circ)] - (0.282\text{kg})g(300\text{mm}) \cos (0^\circ) \\ &= 145,048\text{Nmm} \end{aligned} \quad (22)$$

Table 5 shows the torque values obtained for two static calculation types. The first is when the normal forces are assumed to be a quarter of the robot weight (as if one leg is off the ground). The second is using the worst case method outlined previously where torques are calculated based on only three legs touching the ground. It can be seen that the highest torques appear in legs A and B. These are considered as determined in Section 3.3.

Table 5: Leg Joint Torques Based on Two Different Calculated Normal Forces

Method	Leg	Knee Torque [Nmm]	Hip Torque [Nmm]
Equal Normal Forces	All	36,000	86,000
Worst Case Normal Forces	A	60,000	145,000
	B	60,000	145,000
	C	30,000	72,000
	D	41,000	100,000
	E	30,000	72,000

5.3 Generalized Dynamic Equation of Motion

For both the static dynamic case where the legs are moving, the joint torques can be found by developing an inertial matrix, force and gravity matrices, and using them in the dynamic

equation developed in the Robotics course, MCG4134 [7]. The final form, following derivations described in Appendix A.2 and for an arbitrary leg i shown in Figure 12 with joint torques consistent with Figures 10 and 11, is equation 23.

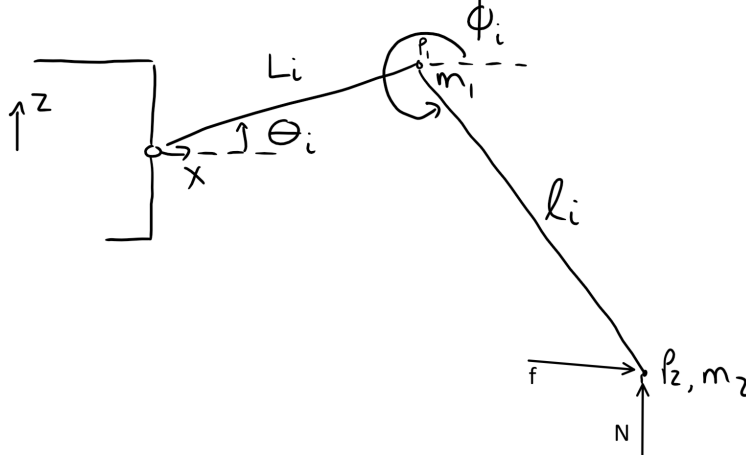


Figure 12: Side View of Leg i

$$\begin{aligned}
 & \begin{bmatrix} (m_1 + m_2)L^2 & m_2\ell L \cos(\theta - \phi) \\ m_2\ell L \cos(\theta - \phi) & m_2\ell^2 \end{bmatrix} \begin{bmatrix} \ddot{\theta} \\ \ddot{\phi} \end{bmatrix} + g \begin{bmatrix} (m_1 + m_2)L \cos \theta + m_2\ell \cos \theta \\ m_2\ell \cos \phi \end{bmatrix} \\
 & + N \begin{bmatrix} L \cos \theta + \ell \cos \phi \\ \ell \cos \phi \end{bmatrix} + f \begin{bmatrix} L \sin \theta + \ell \sin \phi \\ \ell \sin \phi \end{bmatrix} = \begin{bmatrix} \tau_1 \\ \tau_2 \end{bmatrix} \quad (23)
 \end{aligned}$$

where m_1 and m_2 are the masses of the linkages and joints (moved to the most distal point of the linkage), N is the normal force at the foot, f is the friction force at the foot (and encompasses wind, chassis acceleration, and other external forces parallel the ground), and τ_1 and τ_2 are the joint torques at the hip and knee respectively. This approach is conservative, as the actual inertial matrix would contain mass values closer to the center of the linkages. It also simplifies the mass moment of inertia calculations presented in Appendix A.1. An example with leg A is shown below, where the chassis was assumed to be accelerating forward at a rate of $a = 0.5m/s^2$ on a flat surface with no wind. The maximum static friction force $f_{max} = \mu N$ is assumed to be superior to the reaction at the foot to allow for the chassis to move forward with $F = ma = f$ (no slipping). Assuming an even distribution of load and three legs making contact with the ground, the friction force per leg is thus one third of the force required to move the the chassis.

$$f = \frac{ma}{3} = \frac{(63\text{kg})(0.5m/s^2)}{3\text{legs}} = 10.62N \quad (24)$$

$$\begin{aligned}
& \left[\begin{array}{cc} (0.836\text{kg} + 0.532\text{kg})(300\text{mm})^2 & (0.532\text{kg})(300\text{mm})(300\text{mm}) \cos(0^\circ - 315^\circ) \\ 0.532\text{kg}(300\text{mm})(300\text{mm}) \cos(0^\circ - 315^\circ) & 0.532\text{kg}(300\text{mm}) \end{array} \right] \begin{bmatrix} (5\text{rad}/s^2) \\ (5\text{rad}/s^2) \end{bmatrix} \\
& + (9.81\text{m}/s^2) \left[\begin{array}{c} (0.836\text{kg} + 0.532\text{kg})(300\text{mm}) \cos(0^\circ) + 0.532\text{kg}(300\text{mm}) \cos(0^\circ) \\ m_2(300\text{mm}) \cos(315^\circ) \end{array} \right] \\
& + (285\text{N}) \left[\begin{array}{c} (300\text{mm}) \cos(0^\circ) + (300\text{mm}) \cos(315^\circ) \\ (300\text{mm}) \cos(315^\circ) \end{array} \right] \\
& + (10.62\text{N}) \left[\begin{array}{c} (300\text{mm}) \sin(0^\circ) + (300\text{mm}) \sin(315^\circ) \\ (300\text{mm}) \sin(315^\circ) \end{array} \right] = \begin{bmatrix} (150,000\text{Nmm}) \\ (60,000\text{Nmm}) \end{bmatrix} \\
& \hspace{15em} (25)
\end{aligned}$$

Tables 6 and 7 show the values obtained for all other leg following the same equation at the given acceleration, for both forward and backwards motion. These tables can be compared with Table 5; all torques are very similar and very close in value.

Table 6: Leg Joint Torque Based on Generalized Equation of Motion with Forward Acceleration

Method	Leg	Knee Torque [Nmm]	Hip Torque [Nmm]
Generalized Equation of Motion	A	60,000	149,000
	B	60,000	152,000
	C	33,000	80,000
	D	44,000	108,000
	E	33,000	80,000

Table 7: Leg Joint Torque Based on Generalized Equation of Motion with Backward Acceleration

Method	Leg	Knee Torque [Nmm]	Hip Torque [Nmm]
Generalized Equation of Motion	A	65,000	155,000
	B	65,000	155,000
	C	28,000	76,000
	D	40,000	104,000
	E	28,000	75,000

5.4 Stability Analysis and Slopes

The stability analysis allows to determine the area of stability of the robot. Stability triangles show the limit and area of stability of the robot when standing on three of the five legs. By linking legs in combinations as seen in section 5.1, a stability diagram is created as shown in Figure 13. The centre of mass must be located at all times in the diamond shaped area located in the middle of the robot. This will ensure a constant stability with whichever combination of legs.

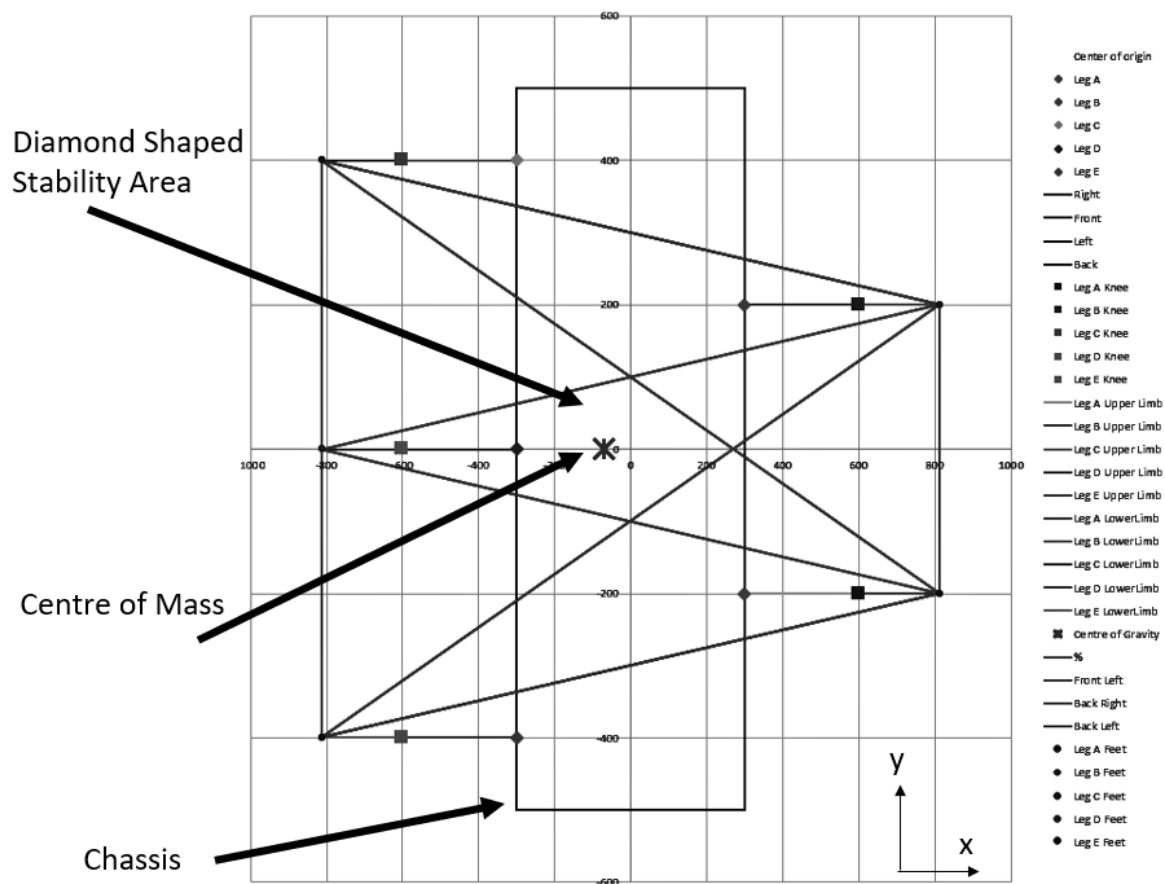


Figure 13: Centre of Mass and Diamond Shaped Stability Area

To assess the robots' stability on slopes, rotational matrices were used around X, Y, and

Z [7]. These are shown here:

$$R_x = \begin{bmatrix} 1 & 0 & 0 \\ 0 & \cos \theta & -\sin \theta \\ 0 & \sin \theta & \cos \theta \end{bmatrix} \quad (26)$$

$$R_y = \begin{bmatrix} \cos \phi & 0 & \sin \phi \\ 0 & 1 & 0 \\ -\sin \phi & 0 & \cos \phi \end{bmatrix} \quad (27)$$

$$R_z = \begin{bmatrix} \cos \sigma & -\sin \sigma & 0 \\ \sin \sigma & \cos \sigma & 0 \\ 0 & 0 & 1 \end{bmatrix} \quad (28)$$

The fixed frame's Z direction is always parallel and in the opposite direction to the gravitational force. The fixed frame is defined by $[X \ Y \ Z]^{-1}$. The robot's frame is defined by $[x \ y \ z]^{-1}$

Rotation from x to z R_z^0 is defined as:

$$R_z^x = R_z R_y R_x \quad (29)$$

Thus, to obtain the robot's location, the following equation is used:

$$\begin{bmatrix} x \\ y \\ z \end{bmatrix} = R_z^x \begin{bmatrix} X \\ Y \\ Z \end{bmatrix} \quad (30)$$

Using equation 30, it was possible to model every component of the robot according to the rotations. Using the stability triangles, the maximum slope angle can be determined. The figures 14, 15, 16, 17 shows the robot's center of mass at different locations depending on the slope. The center of mass is the star, which should always be located within the area of stability. It should be noted that the centre of mass itself is not moving, even though it looks like it on the images. The shift between the stability area and centre of mass is created due to their difference in height.

An example using the position of centre of mass is as follows at 20 degrees around x:

$$\begin{bmatrix} x \\ y \\ z \end{bmatrix} = \begin{bmatrix} 1 & 0 & 0 \\ 0 & 0.940 & -0.342 \\ 0 & 0.342 & 0.940 \end{bmatrix} \begin{bmatrix} 740\text{mm} \\ 400\text{mm} \\ 221\text{mm} \end{bmatrix} = \begin{bmatrix} 740\text{mm} \\ 300\text{mm} \\ 344\text{mm} \end{bmatrix} \quad (31)$$

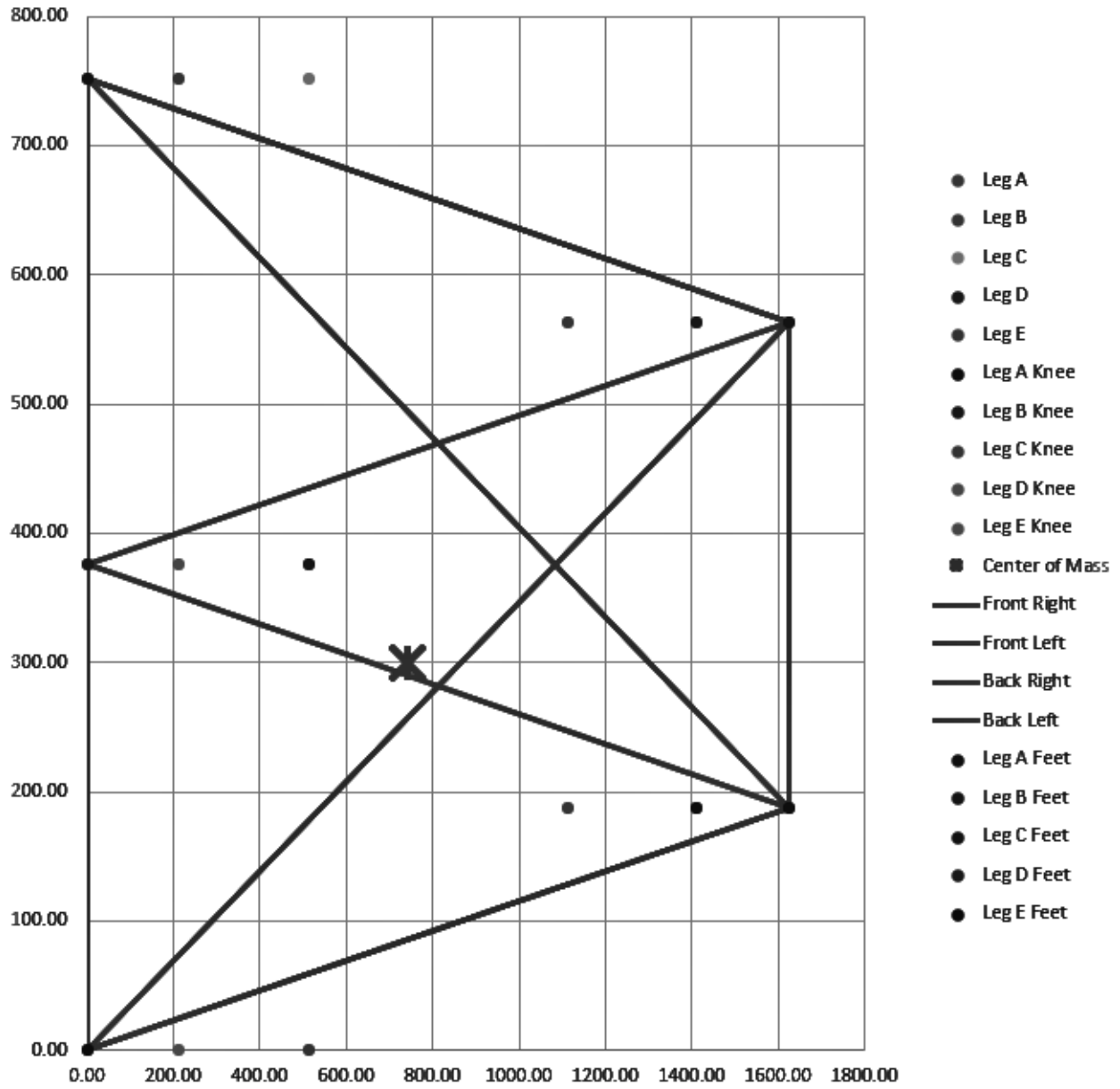


Figure 14: Rotation Around X by 20°

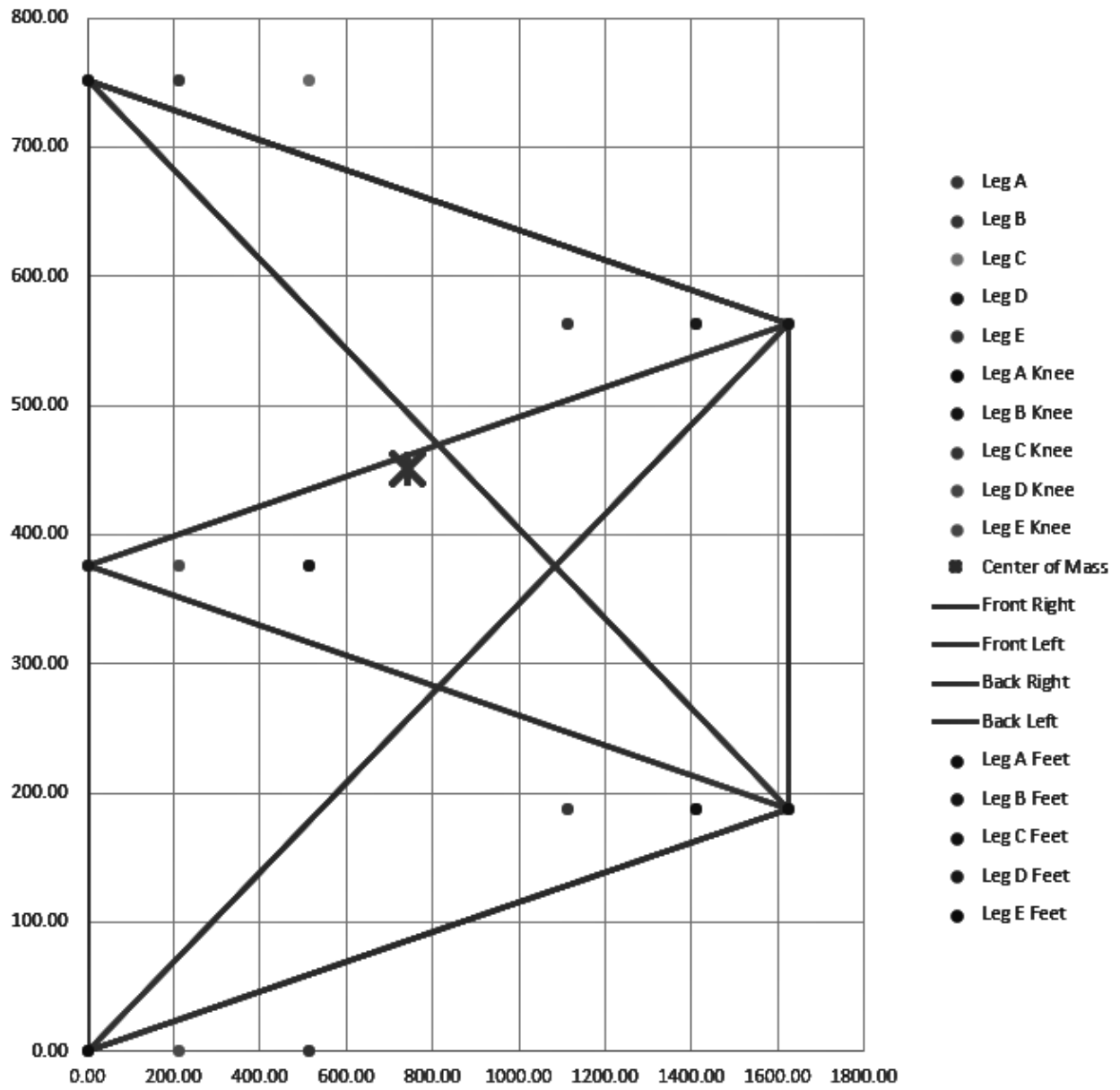


Figure 15: Rotation Around X by -20°

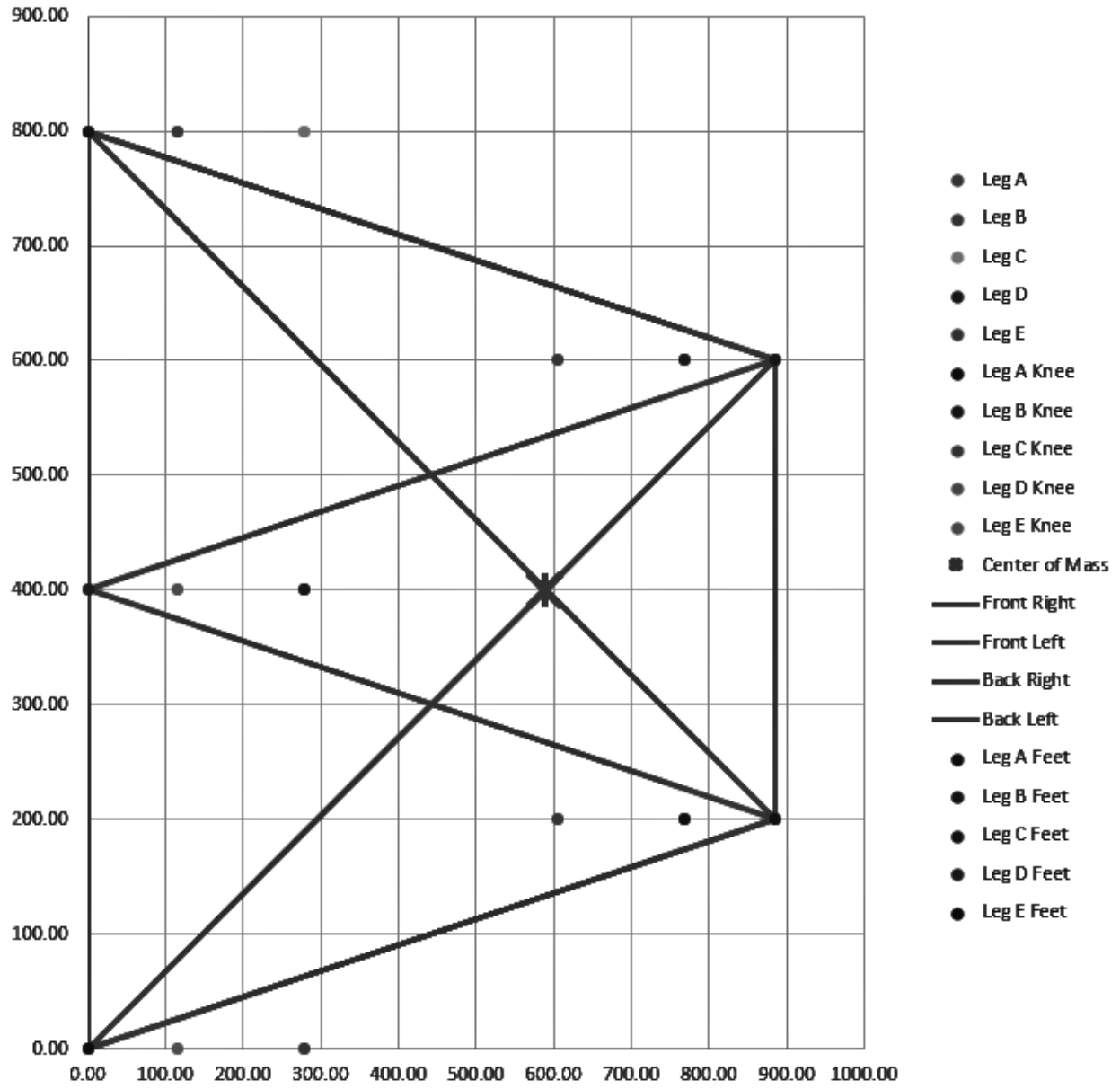


Figure 16: Rotation Around Y by 57°

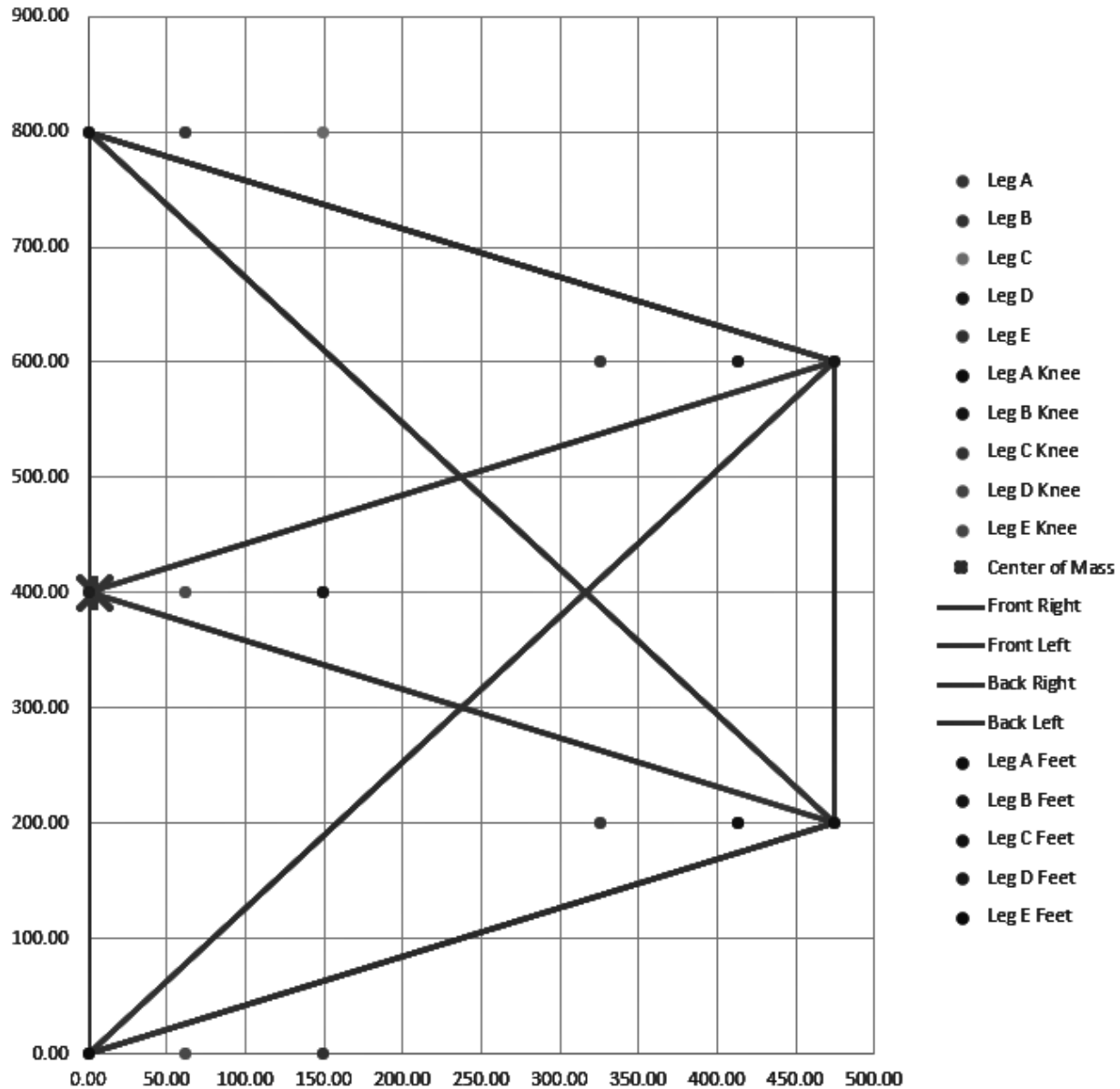


Figure 17: Rotation Around Y by -73°

5.5 Drag Force from Wind

Another external force to consider is the drag force acting on the robot from the wind. Strong winds are common on the waterfront and have the potential to flip the crab over if its weight is not sufficient to keep it on the ground. Based on last year's wind speed data, Ottawa experienced a maximum wind speed of 50 km/h (13.89 m/s) and a maximum gust of 73 km/h (20.78 m/s) in September 2018, which coincides with the tornadoes that occurred

in the region [8]. To calculate the drag force acting on the robot, the drag coefficient C_D is obtained from Figure 25 in Appendix A.4. The value obtained is $C_D = 1.3$ based on the robot's width, depth, and height given in Table 4. For that case to be valid, the Reynold's number should be approximately 10^5 . The equation below is used to calculate the Reynold's number for wind velocity U of $20.28m/s$, a characteristic length D (height h) of $0.2m$, and a kinematic viscosity ν of $1.426 \times 10^{-5} m^2/s$ for air at $10^\circ C$ and $1atm$ [9][10].

$$Re = \frac{UD}{\nu} = \frac{(20.28m/s)(0.2m)}{1.426 \times 10^{-5} m^2/s} = 2.84 \times 10^5 \quad (32)$$

Since 2.84×10^5 has the same order of magnitude as 10^5 , the case used is assumed to be valid. Then, the drag force is calculated using the following equation [9].

$$F_D = \frac{1}{2} \rho U^2 C_D A = \frac{1}{2} (1.246 kg/m^3) (20.28 m/s)^2 (1.3) (1m) (0.2m) = 66.62 N \quad (33)$$

where ρ is the density of the air at $10^\circ C$ and A is the reference area of the chassis ($A = bD = wh$) [10].

The worst case scenario for the robot with drag force is in the situation on a inclined slope of 20 degrees rotated with respect to the y axis as illustrated in Figure 18. The drag force required to flip the robot is calculated using Figure 19. The equations are as follows:

$$d = -H \sin \theta + D \cos \theta = -(350mm) \sin(20 \text{ deg}) + (300mm) \cos(20 \text{ deg}) = 162mm \quad (34)$$

$$h = H \cos \theta + D \sin \theta = (350mm) \cos(20 \text{ deg}) + (300mm) \sin(20 \text{ deg}) = 431mm \quad (35)$$

$$\sum M = 0 = F_D h - mgd \rightarrow F_D = \frac{mgd}{h} \quad (36)$$

$$F_D = \frac{mgd}{h} = \frac{(63.6928kg)(9.81m/s^2)(256mm)}{(468mm)} = 235N \quad (37)$$

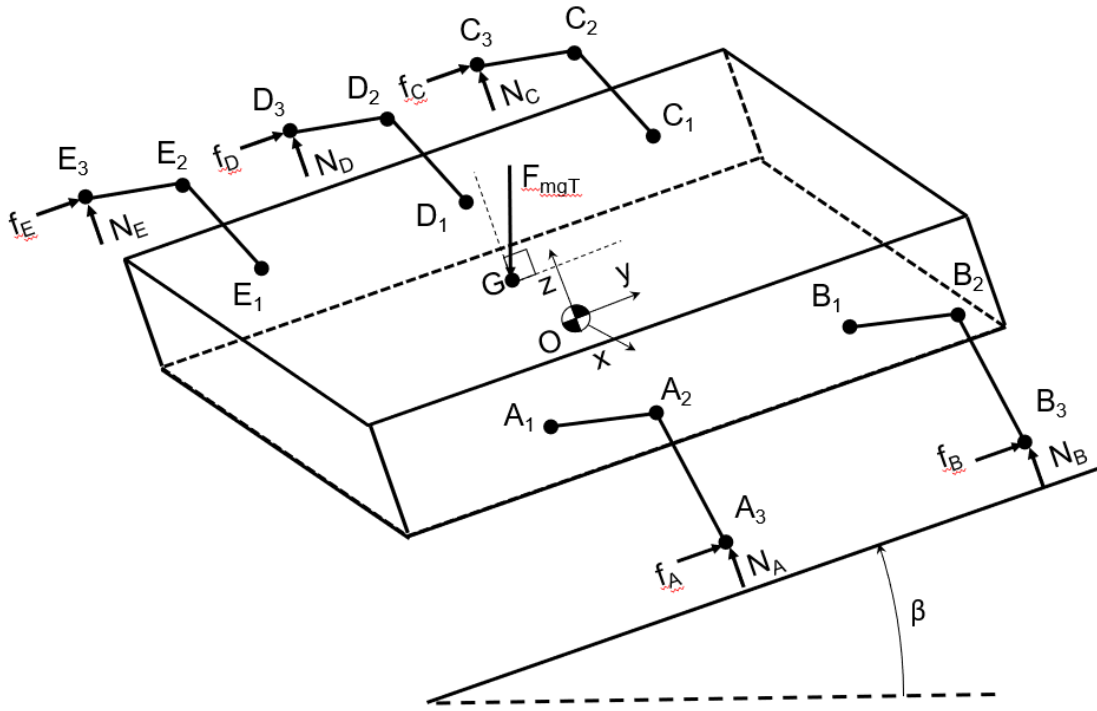


Figure 18: FBD of Whole Robot on a Slope

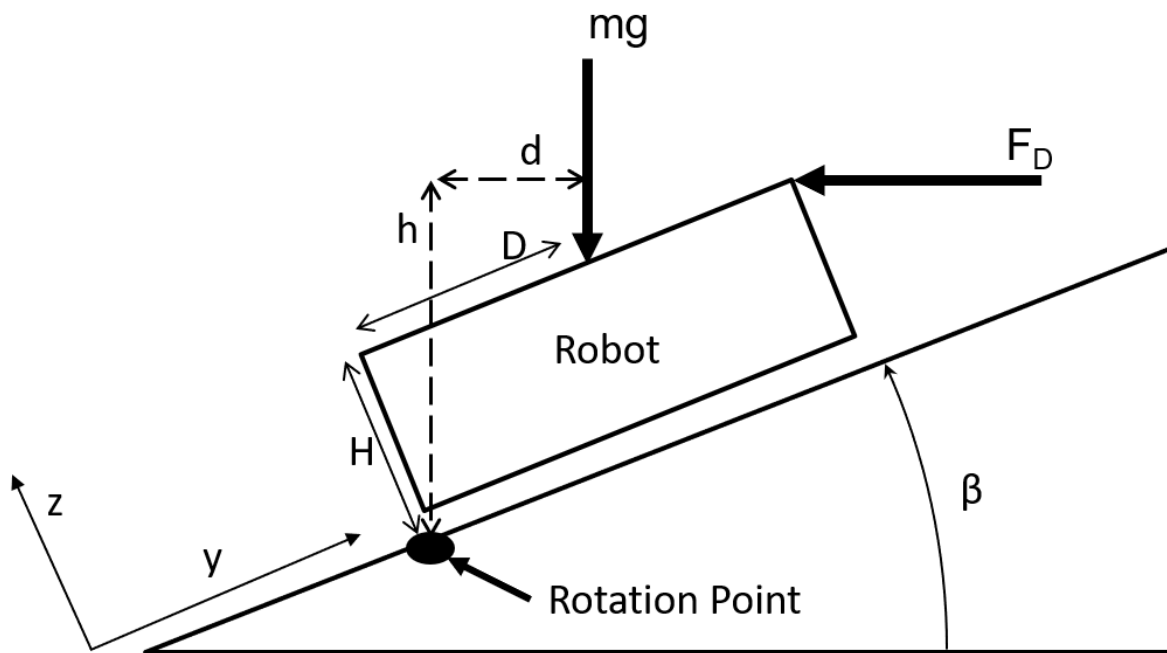


Figure 19: Drag Force Worst Case Scenario

6 References

- [1] Harmonic Drive, “CSD-2a Component Set | Harmonic Drive.” [Online]. Available: <https://www.harmonicdrive.net/products/component-sets/cup-type/csd-2a>
- [2] maxon motor, “EC60 flat 60mm, brushless, 100 W, with Hall sensors.” [Online]. Available: https://www.maxongroup.com/maxon/view/catalog?etcc_med=ID+Teaser&etcc_cmp=ID-Teaser-Rebrush-Homepage&etcc_cu=onsite&etcc_var=%5bcom%5d%23en%23_d_&etcc_plc=home
- [3] Voltaplex, “6s–16s (22.2v–74v, Adjustable) 100a max. BMS Battery Management System for Lithium-ion Battery Pack with Balancing and Communication.” [Online]. Available: <https://voltaplex.com/22-2v-59-2v-pcb-bms-battery-management-system-for-lithium-ion-battery-pack>
- [4] DigiKey Electronics, “Battery Life Calculator | DigiKey Electronics.” [Online]. Available: <https://www.digikey.com/en/resources/conversion-calculators/conversion-calculator-battery-life>
- [5] Panasonic Industrial Devices, “Specifications for NCR18650bd.” [Online]. Available: https://b2b-api.panasonic.eu/file_stream/pids/fileversion/3445
- [6] 18650batterystore, “18650 Batteries - Rechargeable Lithium Ion | 18650 Battery Store.” [Online]. Available: <https://www.18650batterystore.com/18650-Batteries-s/106.htm>
- [7] A. Al-Jarrah, *MCG4134: Robot Design and Control*, Jan. 2019.
- [8] WeatherStats, “Wind Speed - Hourly data for Ottawa (Kanata - Orléans),” 2019. [Online]. Available: https://ottawa.weatherstats.ca/charts/wind_speed-hourly.html
- [9] B. R. Munson, D. F. Young, T. H. Okiishi, and W. W. Huebsch, *Fundamentals of Fluid Mechanics*, 6th ed. John Wiley & Sons, Inc, 2009.
- [10] Engineers Edge, “Viscosity of Air, Dynamic and Kinematic,” 2019. [Online]. Available: https://www.engineersedge.com/physics/viscosity_of_air_dynamic_and_kinematic_14483.htm
- [11] Wikipedia, “List of moments of inertia,” Sep. 2019, page Version ID: 916773550. [Online]. Available: https://en.wikipedia.org/w/index.php?title=List_of_moments_of_inertia&oldid=916773550

- [12] B. Ferdinand, R. Johnston, and D. Mazurek, “Mass Moments of Inertia,” in *Vector Mechanics for Engineers: Statics and Dynamics*, 11th ed. McGraw-Hill, 2016, pp. 532–536.
- [13] Engineers Edge, “Area Moment of Inertia Section Properties of Square Tube at Center Calculator.” [Online]. Available: https://www.engineersedge.com/calculators/section_square_case_4.htm

A Additional Material

A.1 Mass Moment of Inertia of Square Tube

All moments of inertia are calculated assuming constant density ρ . The thigh linkage is modeled as a cylindrical or square tube (subject to change). In the case of a cylindrical tube, the moment of inertia around an axis as shown in Figure 20 takes either of the following forms [11]

$$I = \frac{\pi \rho h}{12} (3(r_2^4 - r_1^4) + h^2(r_2^2 - r_1^2)) \tag{38}$$

$$I = \frac{1}{12} m (3(r_2^2 + r_1^2) + 4h^2) \tag{39}$$

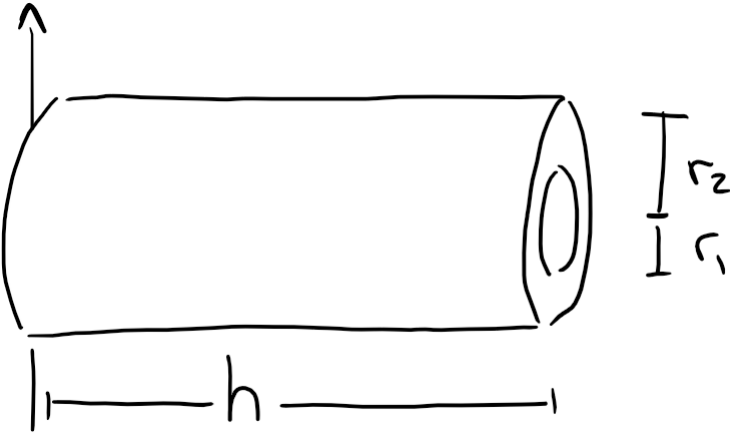


Figure 20: Mass Moment of Inertia of Cylindrical Tube

In the case of a square tube, the general formula is not readily available and must be derived. The derivation follows the variables outlined in Figure 21.

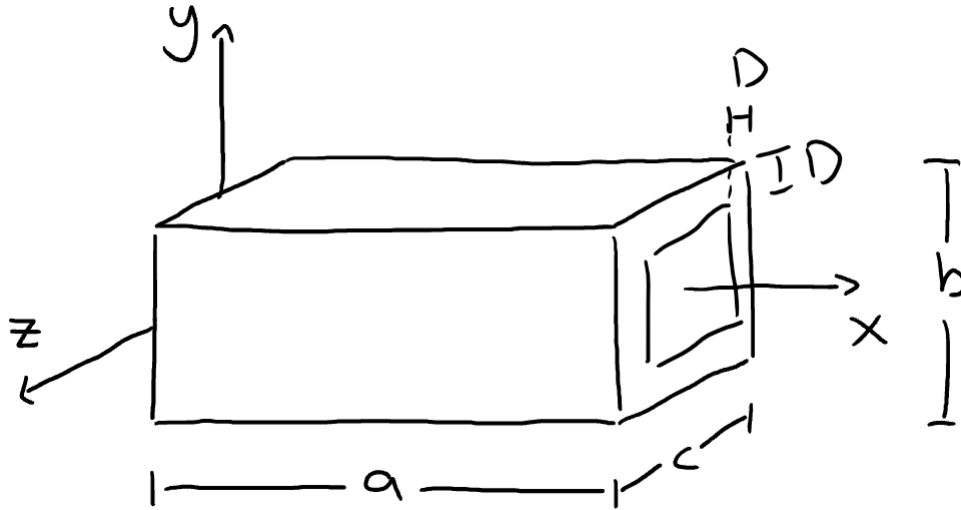


Figure 21: Mass Moment of Inertia of Square Tube

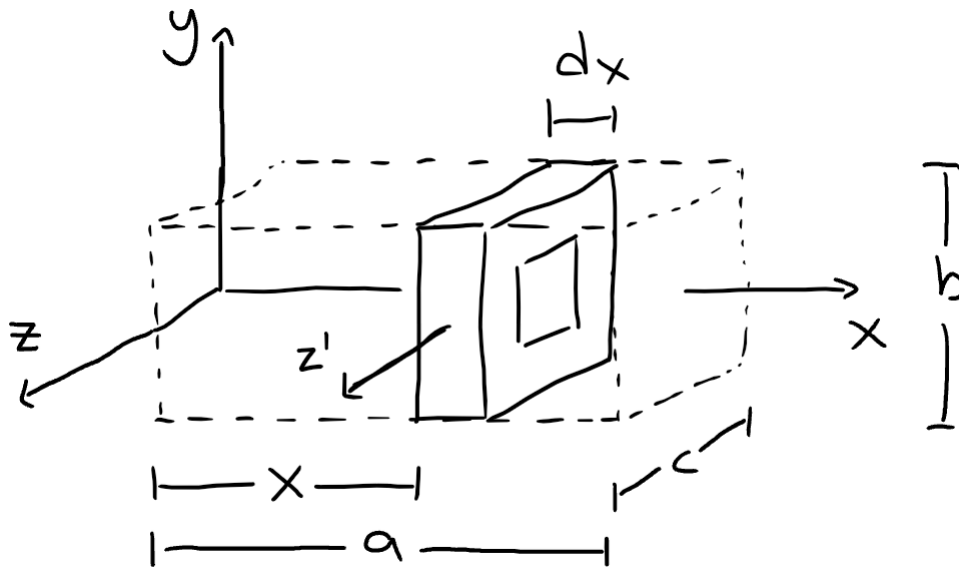


Figure 22: Mass Moment of Inertia of Square Tube - Slab view

To compute the mass moment of inertia of a square tube, we must first determine the differential mass of a slab shown in Figure 22

$$dm = \rho(bc - [(c - 2D)(b - 2D)])dx = \rho(2(b + c)D - 4D^2)dx \quad (40)$$

We then find the differential mass moment of inertia relative to the local axis z' [12]

$$dI_{z'} = \rho dx I_{z',area} = \rho dx \frac{cb^3 - (c - 2D)(b - 2D)^3}{12} \quad (41)$$

where $I_{z',area}$ is the area moment of inertia (or second moment of inertia) of the slab face [13]. The differential mass moment of inertia relative to the global z axis can thus be found using the parallel axis theorem [12]

$$dI_z = dI_{z'} + x^2 dm \quad (42)$$

$$dI_z = \rho dx I_{z',area} + x^2 dm \quad (43)$$

$$dI_z = \rho I_{z',area} dx + x^2 \rho [2(b + c)D - 4D^2] dx \quad (44)$$

$$dI_z = \rho (I_{z',area} + [2(b + c)D - 4D^2] x^2) dx \quad (45)$$

Finally, the expression is integrated with respect to a , giving the mass moment of inertia of the tube

$$I_z = \rho \int_0^a I_{z',area} + [2(b + c)D - 4D^2] x^2 dx \quad (46)$$

$$I_z = \rho a [I_{z',area} + \frac{1}{3}(2(b + c)D - 4D^2)a^2] \quad (47)$$

$$I_z = \rho a \left(\frac{cb^3 - (c - 2D)(b - 2D)^3}{12} + \frac{1}{3}(2(b + c)D - 4D^2)a^2 \right) \quad (48)$$

In the case of a square tube, $b = c$, and so the expression becomes

$$I_z = \rho a \left(\frac{b^4 - (b - 2D)^4}{12} + \frac{1}{3}(4bD - 4D^2)a^2 \right) \quad (49)$$

The mass moment of inertia of composite bodies (composed of multiple bodies) can be calculated as the sum of all mass moments of inertia of the composite body, relative to the axis around which the inertia is being measured.

$$I_{compositebody} = \sum_i I_i \quad (50)$$

The moment of inertia around the hip, for example, would be:

$$I_{hip} = I_{thigh} + I_{knee} + I_{tibia} + I_{foot} \quad (51)$$

Alternatively, a simple and conservative approximation of the linkage moments of inertia can be found using the inertia matrix in Subsection 5.3.

A.2 Generalized Equation of Motion

The following derivation allows for a single vector equation that provides the resulting joint torques for a given configuration and acceleration. A side view of the leg i is shown in Figure 23. From now on, the letter i shall be dropped from all notation to speed up equation writing; all variables are still with respect to leg i .

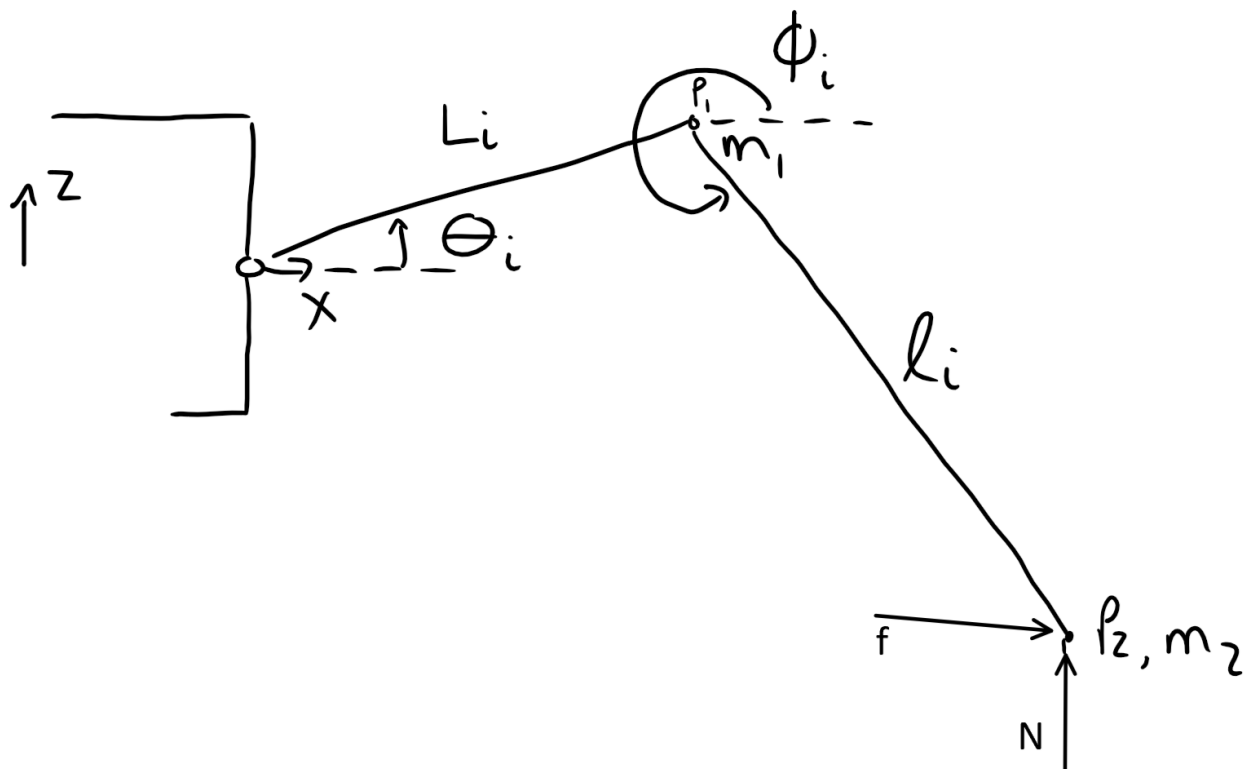


Figure 23: Side View of Leg i

The positions of points P_1 and P_2 in x and z are given in vector form

$$P_1 = \begin{bmatrix} L \cos \theta \\ L \sin \theta \end{bmatrix} \quad (52)$$

$$P_2 = \begin{bmatrix} L \cos \theta + \ell \cos \phi \\ L \sin \theta + \ell \sin \phi \end{bmatrix} \quad (53)$$

After deriving once

$$P_1 = \begin{bmatrix} -L\dot{\theta} \sin \theta \\ L\dot{\theta} \cos \theta \end{bmatrix} \quad (54)$$

$$P_2 = \begin{bmatrix} -L\dot{\theta} \sin \theta - \ell\dot{\phi} \sin \phi \\ L\dot{\theta} \cos \theta + \ell\dot{\phi} \cos \phi \end{bmatrix} \quad (55)$$

In explicit matrix form:

$$P_1 : \begin{bmatrix} \dot{x} \\ \dot{z} \end{bmatrix} = \begin{bmatrix} -L \sin \theta & 0 \\ L \cos \theta & 0 \end{bmatrix} \begin{bmatrix} \dot{\theta} \\ \dot{\phi} \end{bmatrix} \quad (56)$$

$$P_2 : \begin{bmatrix} \dot{x} \\ \dot{z} \end{bmatrix} = \begin{bmatrix} -L \sin \theta & -\ell \sin \phi \\ L \cos \theta & \ell \cos \phi \end{bmatrix} \begin{bmatrix} \dot{\theta} \\ \dot{\phi} \end{bmatrix} \quad (57)$$

Where the 4×4 matrices are Jacobians J_1 and J_2 . The inertia matrix is given by

$$M = m_1 J_1^T J_1 + m_2 J_2^T J_2 = [kg][m][m] + [kg][m][m] \quad (58)$$

This matrix approximates the inertial component of the necessary motor torques conservatively by approximating the entire mass of the linkages at the joints. After substituting in 56 and 57, the resulting inertia matrix takes the form

$$M = \begin{bmatrix} (m_1 + m_2)L^2 & m_2\ell L \cos(\theta - \phi) \\ m_2\ell L \cos(\theta - \phi) & m_2\ell^2 \end{bmatrix} \quad (59)$$

The simplification steps between equations 58 and 59 are shown in Figure 24

$$\begin{aligned}
M &= m_1 J_1^T J_1 + m_2 J_2^T J_2 \\
&= m_1 \begin{bmatrix} -L_i \sin \theta_i & L_i \cos \theta_i \\ 0 & 0 \end{bmatrix} \begin{bmatrix} -L_i \sin \theta_i & 0 \\ L_i \cos \theta_i & 0 \end{bmatrix} \\
&\quad + m_2 \begin{bmatrix} -L_i \sin \theta_i & L_i \cos \theta_i \\ -l_i \sin \phi_i & l_i \cos \phi_i \end{bmatrix} \begin{bmatrix} -L_i \sin \theta_i & -l_i \sin \phi_i \\ L_i \cos \theta_i & l_i \cos \phi_i \end{bmatrix} \\
&= m_1 \begin{bmatrix} L_i^2 \sin^2 \theta_i + L_i^2 \cos^2 \theta_i & 0 \\ 0 & 0 \end{bmatrix} + m_2 \begin{bmatrix} L_i^2 \sin^2 \theta_i + L_i^2 \cos^2 \theta_i & l_i \sin \phi_i L_i \sin \theta_i + l_i \cos \phi_i L_i \cos \theta_i \\ l_i \sin \phi_i L_i \sin \theta_i + l_i \cos \phi_i L_i \cos \theta_i & l_i^2 \sin^2 \phi_i + l_i^2 \cos^2 \phi_i \end{bmatrix} \\
&= m_1 \begin{bmatrix} L_i^2 & 0 \\ 0 & 0 \end{bmatrix} + m_2 \begin{bmatrix} L_i^2 & l_i L_i (\sin \phi_i \sin \theta_i + \cos \phi_i \cos \theta_i) \\ l_i L_i (\sin \phi_i \sin \theta_i + \cos \phi_i \cos \theta_i) & l_i^2 \end{bmatrix} \\
&= m_1 \begin{bmatrix} L_i^2 & 0 \\ 0 & 0 \end{bmatrix} + m_2 \begin{bmatrix} L_i^2 & l_i L_i \cos(\theta_i - \phi_i) \\ l_i L_i \cos(\theta_i - \phi_i) & l_i^2 \end{bmatrix} \\
\boxed{M} &= \begin{bmatrix} (m_1 + m_2) L_i^2 & m_2 l_i L_i \cos(\theta_i - \phi_i) \\ m_2 l_i L_i \cos(\theta_i - \phi_i) & m_2 l_i^2 \end{bmatrix}
\end{aligned}$$

Figure 24: Simplification Steps for Inertia Matrix

The generalized equation of motion takes the form

$$M\ddot{\theta} + c(\theta, \dot{\theta}) + \mu(\dot{\theta}^2) + G(\theta) + F(\theta) = \tau \quad (60)$$

where $c(\theta, \dot{\theta})$ is the coriolis effect, $\mu(\dot{\theta}^2)$ is the centrifugal effect, $G(\theta)$ is gravity, $F(\theta)$ is the force applied at the foot and τ is the joint torques. Coriolis and centrifugal forces have been neglected to simplify analysis. $G(\theta)$ is given by

$$G(\theta) = g \begin{bmatrix} (m_1 + m_2)L \cos \theta + m_2 l \cos \theta \\ m_2 l \cos \phi \end{bmatrix} = [m/s^2]([kg][m]) = [Nm] \quad (61)$$

where $g = 9.81m/s^2$. The force matrix $F(\theta)$ is

$$F(\theta) = N \begin{bmatrix} L \cos \theta + l \cos \phi \\ l \cos \phi \end{bmatrix} + f \begin{bmatrix} L \sin \theta + l \sin \phi \\ l \sin \phi \end{bmatrix} = [N][m] \quad (62)$$

where N is the normal force at the foot and f is the friction force at the foot. Friction force in the y plane was neglected as it should not directly impact the joint torques, except through increasing the friction in bearings, etc. Finally, equations 61 and 62 are inserted

into 60 giving the final generalized equation of motion

$$\begin{aligned} & \begin{bmatrix} (m_1 + m_2)L^2 & m_2\ell L \cos(\theta - \phi) \\ m_2\ell L \cos(\theta - \phi) & m_2\ell \end{bmatrix} \begin{bmatrix} \ddot{\theta} \\ \ddot{\phi} \end{bmatrix} + g \begin{bmatrix} (m_1 + m_2)L \cos \theta + m_2\ell \cos \theta \\ m_2\ell \cos \phi \end{bmatrix} \\ & + N \begin{bmatrix} L \cos \theta + \ell \cos \phi \\ \ell \cos \phi \end{bmatrix} + f \begin{bmatrix} L \sin \theta + \ell \sin \phi \\ \ell \sin \phi \end{bmatrix} = \begin{bmatrix} \tau_1 \\ \tau_2 \end{bmatrix} \end{aligned} \quad (63)$$

where τ_1 and τ_2 are the joint torques for the hip and knee, respectively.

A.3 Force at Feet

These equations were first tried to calculate the force at every feet of the robot, however after calculation it was determined to be a statically indeterminate system.

$$\sum F_z = 0 = N_A + N_B + N_C + N_D + N_E - mg \quad (64)$$

$$\sum M_{x_A} = 0 = -N_E r_{EA_y} + N_D r_{DA_y} + N_B r_{BA_y} + N_C r_{CA_y} - mgr_{gA_y} \quad (65)$$

$$\sum M_{x_E} = 0 = N_A r_{AE_y} N_D r_{DE_y} + N_B r_{BE_y} + N_C r_{CE_y} - mgr_{gE_y} \quad (66)$$

$$\sum M_{y_A} = 0 = N_E r_{EA_x} + N_D r_{DA_x} + N_C r_{CA_x} - mgr_{gA_x} \quad (67)$$

$$\sum M_{y_B} = 0 = N_E r_{EB_x} + N_D r_{DB_x} + N_C r_{CB_x} - mgr_{gB_x} \quad (68)$$

What if there is force in different directions (Complete 3D), must look at matrices?

$$M_j = \sum (r_i \times N_i) + mg \quad (69)$$

$$M_{j_x} = \sum (r_{i_y} N_{i_z} - r_{i_z} N_{i_y}) + \dots \quad (70)$$

$$M_{j_y} = \sum (r_{i_z} N_{i_x} - r_{i_x} N_{i_z}) + \dots \quad (71)$$

$$M_{j_z} = \sum (r_{i_x} N_{i_y} - r_{i_y} N_{i_x}) + \dots \quad (72)$$

A.4 Drag Coefficients

The drag coefficient acting on the robot was obtained with Figure 25. The most appropriate shape is the rectangle with the values $D = h = 200mm$, $l = d = 600mm$, and $b = w = 1000mm$. Therefore, we obtain a ratio of $l/D = d/h = 600mm/200mm = 3$ and based on the table from Figure 25, $C_D = 1.3$. Finally, the reference area $A = bD = wh = (1m)(0.2m) = 0.2m^2$.

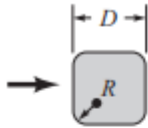

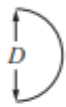
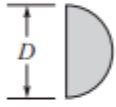

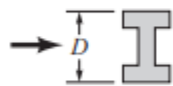
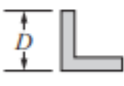
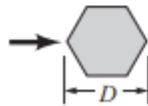
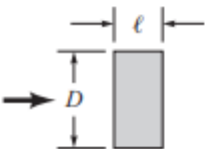
Shape	Reference area A ($b = \text{length}$)	Drag coefficient $C_D = \frac{\mathcal{Q}}{\frac{1}{2}\rho U^2 A}$	Reynolds number $Re = \rho U D / \mu$																		
 <p>Square rod with rounded corners</p>	$A = bD$	<table border="1"> <thead> <tr> <th>R/D</th> <th>C_D</th> </tr> </thead> <tbody> <tr><td>0</td><td>2.2</td></tr> <tr><td>0.02</td><td>2.0</td></tr> <tr><td>0.17</td><td>1.2</td></tr> <tr><td>0.33</td><td>1.0</td></tr> </tbody> </table>	R/D	C_D	0	2.2	0.02	2.0	0.17	1.2	0.33	1.0	$Re = 10^5$								
R/D	C_D																				
0	2.2																				
0.02	2.0																				
0.17	1.2																				
0.33	1.0																				
 <p>Rounded equilateral triangle</p>	$A = bD$	<table border="1"> <thead> <tr> <th>R/D</th> <th colspan="2">C_D</th> </tr> <tr> <td></td> <th>→</th> <th>←</th> </tr> </thead> <tbody> <tr><td>0</td><td>1.4</td><td>2.1</td></tr> <tr><td>0.02</td><td>1.2</td><td>2.0</td></tr> <tr><td>0.08</td><td>1.3</td><td>1.9</td></tr> <tr><td>0.25</td><td>1.1</td><td>1.3</td></tr> </tbody> </table>	R/D	C_D			→	←	0	1.4	2.1	0.02	1.2	2.0	0.08	1.3	1.9	0.25	1.1	1.3	$Re = 10^5$
R/D	C_D																				
	→	←																			
0	1.4	2.1																			
0.02	1.2	2.0																			
0.08	1.3	1.9																			
0.25	1.1	1.3																			
 <p>Semicircular shell</p>	$A = bD$	<table border="1"> <tbody> <tr><td>→</td><td>2.3</td></tr> <tr><td>←</td><td>1.1</td></tr> </tbody> </table>	→	2.3	←	1.1	$Re = 2 \times 10^4$														
→	2.3																				
←	1.1																				
 <p>Semicircular cylinder</p>	$A = bD$	<table border="1"> <tbody> <tr><td>→</td><td>2.15</td></tr> <tr><td>←</td><td>1.15</td></tr> </tbody> </table>	→	2.15	←	1.15	$Re > 10^4$														
→	2.15																				
←	1.15																				
 <p>T-beam</p>	$A = bD$	<table border="1"> <tbody> <tr><td>→</td><td>1.80</td></tr> <tr><td>←</td><td>1.65</td></tr> </tbody> </table>	→	1.80	←	1.65	$Re > 10^4$														
→	1.80																				
←	1.65																				
 <p>I-beam</p>	$A = bD$	2.05	$Re > 10^4$																		
 <p>Angle</p>	$A = bD$	<table border="1"> <tbody> <tr><td>→</td><td>1.98</td></tr> <tr><td>←</td><td>1.82</td></tr> </tbody> </table>	→	1.98	←	1.82	$Re > 10^4$														
→	1.98																				
←	1.82																				
 <p>Hexagon</p>	$A = bD$	1.0	$Re > 10^4$																		
 <p>Rectangle</p>	$A = bD$	<table border="1"> <thead> <tr> <th>l/D</th> <th>C_D</th> </tr> </thead> <tbody> <tr><td>≤ 0.1</td><td>1.9</td></tr> <tr><td>0.5</td><td>2.5</td></tr> <tr><td>0.65</td><td>2.9</td></tr> <tr><td>1.0</td><td>2.2</td></tr> <tr><td>2.0</td><td>1.6</td></tr> <tr><td>3.0</td><td>1.3</td></tr> </tbody> </table>	l/D	C_D	≤ 0.1	1.9	0.5	2.5	0.65	2.9	1.0	2.2	2.0	1.6	3.0	1.3	$Re = 10^5$				
l/D	C_D																				
≤ 0.1	1.9																				
0.5	2.5																				
0.65	2.9																				
1.0	2.2																				
2.0	1.6																				
3.0	1.3																				

Figure 25: Various Drag Coefficients for Two-Dimensional Objects [9]

A.5 Battery Sample Code

Listing 1: Battery dimension calculator - Basic

```
function [x,y,z] = getBatteryDimensionsSingle(number_of_cells ,
    number_of_batteries):

    % Battery dimensions in mm and g
    D = 18.24;
    H = 65.1;

    [cells_per_battery , remainder] = quorem(number_of_cells ,
        number_of_batteries)
    if(remainder != 0):
        cells_per_battery = cells_per_battery + 1;
    end

    % cells are arranged upright, 1 high, with even width and
    length if possible
    cells_wide_square = sqrt(cells_per_battery);
    cells_wide = floor(cells_wide_square);
    cells_long = ceil(cells_wide_square);

    x = cells_wide * D;
    y = cells_long * D;
    z = H;
```

The chassis dimensions could then be found programmatically by multiplying the battery dimensions by some constant (for example, $h_{chassis} = 1.5h_{battery}$, then ensuring that this length is also sufficient to allow the desired range of motion of the leg

A.6 Centre of Mass Calculation

Table 8: Centre of Mass Calculation and Components' Location

Centre of Gravity								
Components	Location x [mm]	Location y [mm]	Location z [mm]	Weight (kg)	mx [kgmm]	my [kgmm]	mz [kgmm]	
Battery 1	-180	200	40	7.7	-1390.0	1544.4	308.9	Total Weight [kg] 63.69
Battery 2	-180	-200	40	7.7	-1390.0	-1544.4	308.9	CG X [mm] -71.68
Battery 3	-180	200	120	7.7	-1390.0	1544.4	926.6	CG Y [mm] 0.02
Battery 4	-180	-200	120	7.7	-1390.0	-1544.4	926.6	CG Z [mm] 71.41
Litter	50	0	175	5.0	250.0	0.0	875.0	
Litter Arm	300	0	0	6.0	1800.0	0.0	0.0	
Chassis Casing	0	0	100	1.9	0.0	0.0	192.8	
NVIDIA Jetson TX2	-200	-180	140	0.1	-17.0	-15.3	11.9	
Raspberry Pi 4	-200	150	140	0.0	-9.2	6.9	6.4	
BMS (8S-16S)	-200	210	140	0.0	-9.2	9.7	6.4	
Leg A Hip	250	-200	50	3.8	960.0	-768.0	192.0	
Leg B Hip	250	200	50	3.8	960.0	768.0	192.0	
Leg C Hip	-250	400	50	3.8	-960.0	1536.0	192.0	
Leg D Hip	-250	0	50	3.8	-960.0	0.0	192.0	
Leg E Hip	-250	-400	50	3.8	-960.0	-1536.0	192.0	
Leg A Knee	600	-200	50	0.1	60.0	-20.0	5.0	
Leg B Knee	600	200	50	0.1	60.0	20.0	5.0	
Leg C Knee	-600	400	50	0.1	-60.0	40.0	5.0	
Leg D Knee	-600	0	50	0.1	-60.0	0.0	5.0	
Leg E Knee	-600	-400	50	0.1	-60.0	-40.0	5.0	

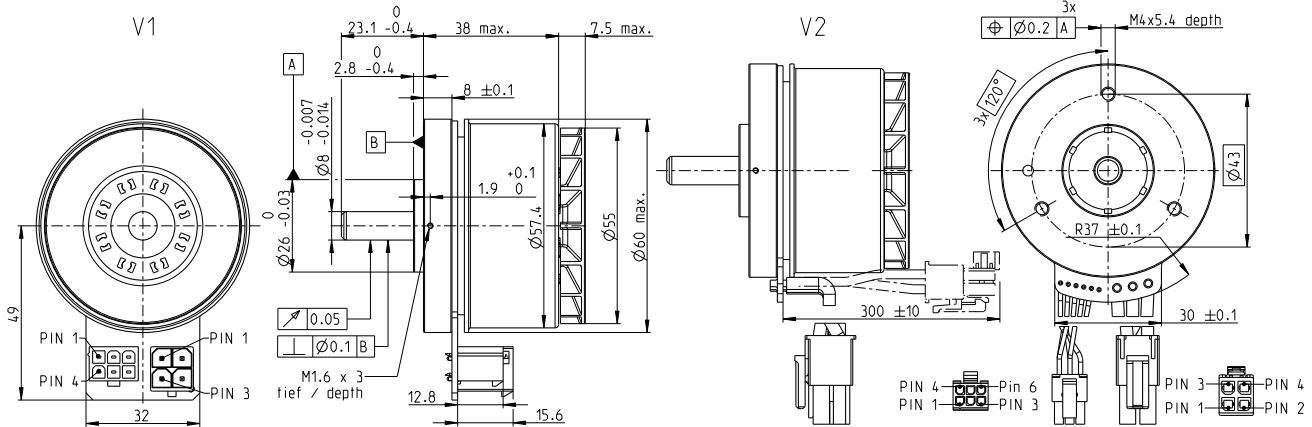
B Data Sheets

EC 60 flat Ø60 mm, brushless, 200 Watt

Ventilated

NEW

maxon flat motor



M 1:2

- Stock program
- Standard program
- Special program (on request)

Part Numbers

	625860	614949	625861
V1 with Hall sensors			
V2 with Hall sensors and cables	647696	642221	647697

Motor Data

Values at nominal voltage		12	24	48
1 Nominal voltage	V	12	24	48
2 No load speed	rpm	3760	4300	4020
3 No load current	mA	815	497	224
4 Nominal speed	rpm	2790	3240	3020
5 Nominal torque (max. continuous torque)	mNm	492	536	577
6 Nominal current (max. continuous current)	A	15.1	9.28	4.6
7 Stall torque ¹	mNm	3340	4300	4870
8 Stall current	A	111	81.9	43.2
9 Max. efficiency	%	83.8	85.2	86.3
Characteristics				
10 Terminal resistance phase to phase	Ω	0.108	0.293	1.11
11 Terminal inductance phase to phase	mH	0.0911	0.279	1.28
12 Torque constant	mNm/A	30	52.5	113
13 Speed constant	rpm/V	318	182	84.8
14 Speed/torque gradient	rpm/mNm	1.14	1.01	0.837
15 Mechanical time constant	ms	9.95	8.83	9.29
16 Rotor inertia	gcm ²	832	832	832

Specifications

Thermal data	
17 Thermal resistance housing-ambient	1.22 K/W
18 Thermal resistance winding-housing	0.843 K/W
19 Thermal time constant winding	9.19 s
20 Thermal time constant motor	44 s
21 Ambient temperature	-40...+100°C
22 Max. winding temperature	+125°C
Mechanical data (preloaded ball bearings)	
23 Max. speed	6000 rpm
24 Axial play at axial load < 12.0 N	0 mm
> 12.0 N	0.14 mm
25 Radial play	preloaded
26 Max. axial load (dynamic)	12 N
27 Max. force for press fits (static) (static, shaft supported)	170 N
28 Max. radial load, 5 mm from flange	8000 N
112 N	

Other specifications

29 Number of pole pairs	7
30 Number of phases	3
31 Weight of motor	360 g

Values listed in the table are nominal.

Connection V1

Pin	V1	V2 (sensors, AWG 24)
Pin 1	Hall sensor 1	Hall sensor 1
Pin 2	Hall sensor 2	Hall sensor 2
Pin 3	V _{Hall} 4.5...24 VDC	Hall sensor 3
Pin 4	Hall sensor 3	GND
Pin 5	GND	V _{Hall} 4.5...24 VDC
Pin 6	N.C.	N.C.

V2 (Motor, AWG 14)

Pin 1	Motor winding 1	Motor winding 1
Pin 2	Motor winding 3	Motor winding 2
Pin 3	Motor winding 2	Motor winding 3
Pin 4		N.C.

Wiring diagram for Hall sensors see p. 47

Connector Part number

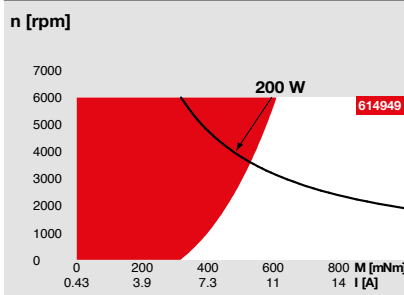
Molex 46015-0606	43025-0600
Molex 76829-0104	171692-0104

Connection cable for V1

Connection cable Universal, L = 500 mm **651900**

¹Calculation does not include saturation effect (p. 57/162)

Operating Range



Comments

Continuous operation

In observation of above listed thermal resistance (lines 17 and 18) the maximum permissible winding temperature will be reached during continuous operation at 25°C ambient. = Thermal limit.

Short term operation

The motor may be briefly overloaded (recurring).

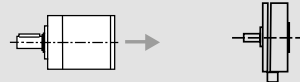
Assigned power rating

maxon Modular System

Details on catalog page 36

Planetary Gearhead

Ø52 mm
4 - 30 Nm
Page 367

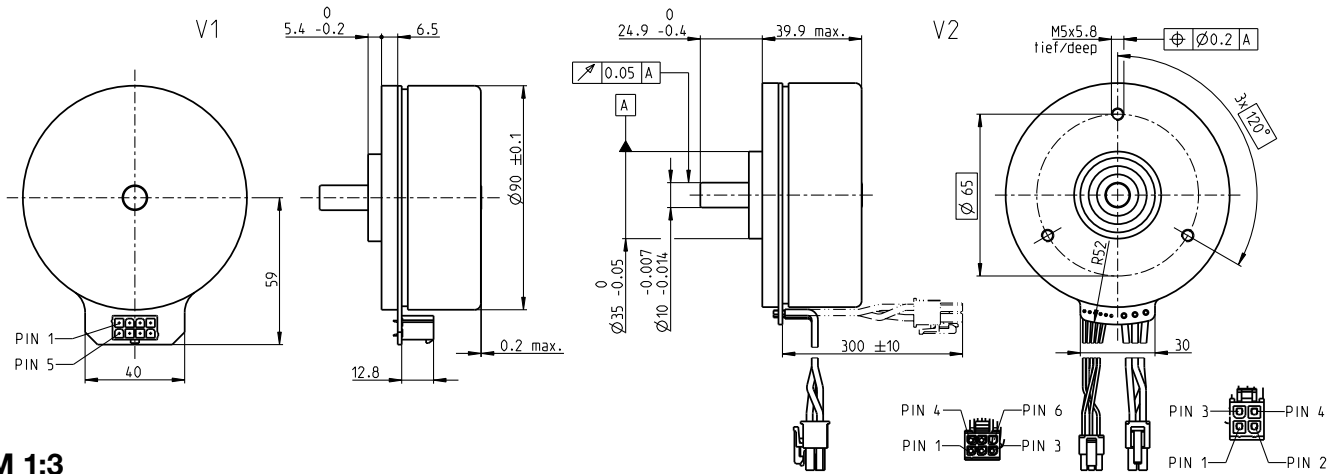


Recommended Electronics:

Notes	Page 36
ESCON Module 50/5	455
ESCON Mod. 50/8 (HE)	456
ESCON 50/5	457
ESCON 70/10	457
DEC Module 50/5	459

EC 90 flat Ø90 mm, brushless, 260 Watt

maxon flat motor



M 1:3

- Stock program
- Standard program
- Special program (on request)

Part Numbers

	500269	500266	500267	500268
V1 with Hall sensors	607325	607326	607327	607328
V2 with Hall sensors and cables				

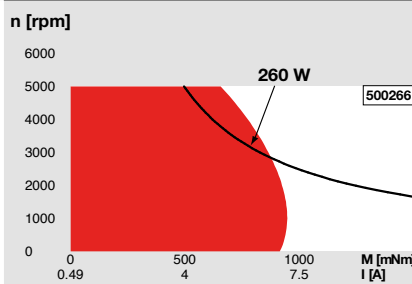
Motor Data

Values at nominal voltage			18	30	48	60
1 Nominal voltage	V		18	30	48	60
2 No load speed	rpm		2110	2080	1960	1980
3 No load current	mA		830	490	278	227
4 Nominal speed	rpm		1790	1780	1670	1690
5 Nominal torque (max. continuous torque)	mNm		1010	988	964	963
6 Nominal current (max. continuous current)	A		12.1	7.06	4.06	3.28
7 Stall torque ¹	mNm		14800	14600	13100	13300
8 Stall current	A		183	107	56.9	46.7
9 Max. efficiency	%		87	87	86	87
Characteristics						
10 Terminal resistance phase to phase	Ω		0.0983	0.28	0.844	1.28
11 Terminal inductance phase to phase	mH		0.133	0.369	1.07	1.63
12 Torque constant	mNm/A		80.7	136	231	286
13 Speed constant	rpm/V		118	70.2	41.3	33.4
14 Speed/torque gradient	rpm/mNm		0.144	0.144	0.151	0.15
15 Mechanical time constant	ms		7.63	7.66	7.99	7.97
16 Rotor inertia	gcm ²		5060	5060	5060	5060

Specifications

- Thermal data**
 - 17 Thermal resistance housing-ambient 1.74 K/W
 - 18 Thermal resistance winding-housing 1.82 K/W
 - 19 Thermal time constant winding 57 s
 - 20 Thermal time constant motor 258 s
 - 21 Ambient temperature -40...+100°C
 - 22 Max. winding temperature +125°C
 - Mechanical data (preloaded ball bearings)**
 - 23 Max. speed 5000 rpm
 - 24 Axial play at axial load 0.14 mm
 - 25 Radial play preloaded
 - 26 Max. axial load (dynamic) 34 N
 - 27 Max. force for press fits (static) (static, shaft supported) 440 N
 - 28 Max. radial load, 10 mm from flange 8000 N
 - 130 N
 - Other specifications**
 - 29 Number of pole pairs 11
 - 30 Number of phases 3
 - 31 Weight of motor 980 g
- Values listed in the table are nominal.

Operating Range



Comments

- Continuous operation**
In observation of above listed thermal resistance (lines 17 and 18) the maximum permissible winding temperature will be reached during continuous operation at 25°C ambient.
= Thermal limit.
- Short term operation**
The motor may be briefly overloaded (recurring).
- Assigned power rating**

- Connection V1**
- Pin 1 Hall sensor 1
- Pin 2 Hall sensor 2
- Pin 3 V_{Hall} 4.5...24 VDC
- Pin 4 Motor winding 3
- Pin 5 Hall sensor 3
- Pin 6 GND
- Pin 7 Motor winding 1
- Pin 8 Motor winding 2
- Connection V2 (sensors, AWG 24)**
- Hall sensor 1
- Hall sensor 2
- Hall sensor 3
- GND
- V_{Hall} 4.5...24 VDC
- N.C.
- V2 (motor, AWG 16)**
- Motor winding 1
- Motor winding 2
- Motor winding 3
- N.C.
- Wiring diagram for Hall sensors see p. 47
- Connector**
- Molex 46015-0806
- Molex 43025-0600
- Molex 39-01-2040
- Connection cable for V1**
- Connection cable Universal, L = 500 mm **339380**
- Connection cable to EPOS4, L = 500 mm **354045**
- ¹Calculation does not include saturation effect (p. 57/162)

maxon Modular System

Details on catalog page 36



Encoder MILE
512 - 6400 CPT,
2 channels
Page 414

- Recommended Electronics:**
- Notes** Page 36
- ESCON Mod. 50/4 EC-S 455
 - ESCON Mod. 50/5 455
 - ESCON Mod. 50/8 (HE) 456
 - ESCON 50/5 457
 - ESCON 70/10 457
 - DEC Module 50/5 459
 - EPOS4 50/5 463
 - EPOS4 Mod./Comp. 50/5 463
 - EPOS4 Mod./Comp. 50/8 465
 - EPOS4 Mod./Comp. 50/15 466
 - EPOS4 70/15 467
 - MAXPOS 50/5 473



FB-25- 100-2- GR



Series	Size	Ratio	Type
FB	25	100	2-GR

FB component set consists of four elements:

- Wave generator, an elliptical bearing assembly
- Flexspline, a non-rigid ring with external teeth
- Circular Spline, rigid internal gear
- Dynamic Spline, rigid internal gear

How it works

Rotation of the Wave Generator imparts a rotating elliptical shape to the Flexspline causing progressive engagement of its external teeth with the internal teeth of the Circular Spline and the Dynamic Spline. The fixed Circular Spline has two more teeth than the Flexspline, thereby imparting relative rotation to the Flexspline at a reduction ratio corresponding to the difference in the number of teeth. With the same number of teeth, the Dynamic Spline rotates with and at the same speed as the Flexspline.

Gear Model Number	FB-25-100-2-GR
--------------------------	-----------------------

Gear Performance Data		
Rated Torque L10	39	Nm
Limit for Average Torque	52	Nm
Limit for Repeated Peak Torque	52	Nm
Limit for Momentary Peak Torque	91	Nm

Gear Performance Data

Backdriving Torque		Nm
Ave. Input Speed	2,500	rpm
Gear Backlash	< 3	arc min
Mass	0.5	kg



FB-40-100-2-GR



Series	Size	Ratio	Type
FB	40	100	2-GR

FB component set consists of four elements:

- Wave generator, an elliptical bearing assembly
- Flexspline, a non-rigid ring with external teeth
- Circular Spline, rigid internal gear
- Dynamic Spline, rigid internal gear

How it works

Rotation of the Wave Generator imparts a rotating elliptical shape to the Flexspline causing progressive engagement of its external teeth with the internal teeth of the Circular Spline and the Dynamic Spline. The fixed Circular Spline has two more teeth than the Flexspline, thereby imparting relative rotation to the Flexspline at a reduction ratio corresponding to the difference in the number of teeth. With the same number of teeth, the Dynamic Spline rotates with and at the same speed as the Flexspline.

Gear Model Number	FB-40-100-2-GR
--------------------------	-----------------------

Gear Performance Data		
Rated Torque L10	157	Nm
Limit for Average Torque	186	Nm
Limit for Repeated Peak Torque	186	Nm
Limit for Momentary Peak Torque	343	Nm

Gear Performance Data

Backdriving Torque		Nm
Ave. Input Speed	2,000	rpm
Gear Backlash	< 3	arc min
Mass	1.8	kg

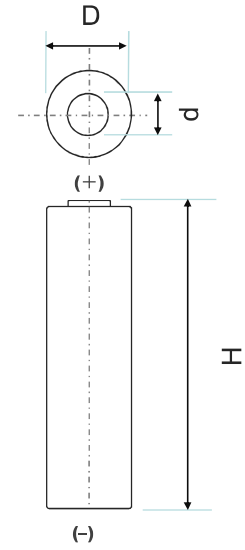
Specifications

Rated capacity ⁽¹⁾		2980mAh	2910mAh
Capacity ⁽²⁾	Minimum	3030mAh	2935mAh
	Typical	3180mAh	3080mAh
Nominal voltage		3.6V	
Charging	Method	CC-CV	
	Voltage	4.20V	4.15V
	Current	Std. 0.3CA	
Weight (max.) Without tube		49.5g	
Temperature	Charge	10 to +45° C	
	Discharge	-20 to +60° C	
	Storage	-20 to +50° C	
Energy density ⁽³⁾	Volumetric	630 Wh/l	615 Wh/l
	Gravimetric	217 Wh/kg	212 Wh/kg

⁽¹⁾ At 20° C ⁽²⁾ At 25° C

⁽³⁾ Energy density is calculated using bare cell dimensions (without tube).

Dimensions



Without tube	H	Max. 65.10mm
	D	Max. 18.25mm
	d	Max. 6.6mm

When designing a pack, refer to the cell's mechanical drawing for precise dimensions.